CERN

www.cern.ch

Main ring quadrupole - vacuum chambers and BPM integration

C. Garion, CERN/TE/VSC

Content:

- Introduction to the FCC-ee vacuum system in the arcs
- UHV connections with Shape Memory Alloy couplers
- Additive manufacturing with gas dynamic cold spray coating
- Other developments
- Summary

FCC-ee vacuum system in the arcs

The FCC-ee Vacuum system has to cope with beam parameters from low-energy (45.6 GeV) high current (1390 mA) version to high-energy (182.5 GeV) low current (5.4 mA) configuration.

Beam Energy E(GeV)	Beam Current I(mA)	Photon Flux F'(ph/s/m)	Dynamic Gas Load Q'(mbar·l/s/m)
45.6	1390	$7.17 \cdot 10^{17}$	$2.90 \cdot 10^{-8}$
80	147	$1.38 \cdot 10^{17}$	$5.58 \cdot 10^{-9}$
120	29	$4.13 \cdot 10^{16}$	$1.67 \cdot 10^{-9}$
182.5	5.4	$1.18 \cdot 10^{16}$	$4.78 \cdot 10^{-10}$

Relevant FCC-ee parameters for the vacuum system design

For the vacuum system, the synchrotron radiation leads to:

- High local heat deposition:
  - The limit is given by 50 MW/beam synchrotron radiation losses (~650 W/m).
- High outgassing:
  - Pressure: low 10^{-9} mbar range.

Layout:

- 2 rings of ~ 100 km.
- Cell length: ~55.9 m.

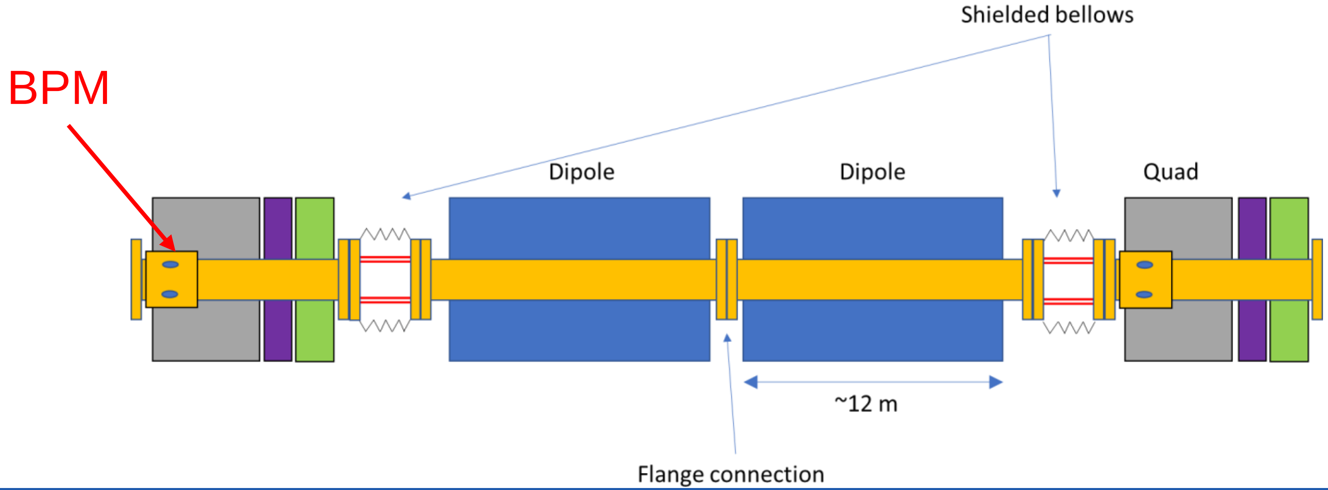

FCC-ee vacuum chambers

Present design as presented in the CDR:

Geometry: Tube with two winglets
2 mm thick, 70 mm ID

Material: Copper

- Good thermal conductivity and low electrical resistivity
- Shielding for the X-Ray synchrotron radiation fan and minimizing the irradiation of machine and tunnel components

Surface treatment: NEG coating

- Distributed pumping speed
- Low SEY
- Quick vacuum conditioning

Lumped SR photon absorber:
Distanced by about 5.8 m

Lumped pump: no need for a systematic installation in vicinity of the absorbers →1 or 2 per cell

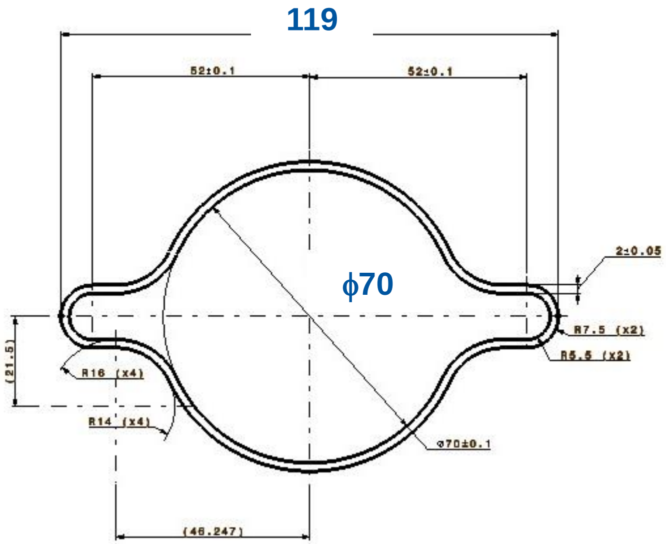

Vacuum chamber prototype cross-section

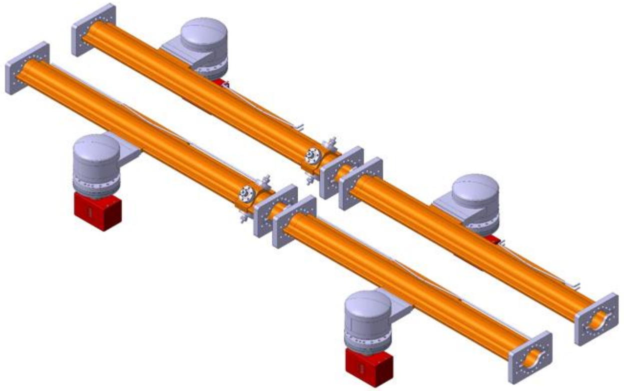

Illustration of vacuum chambers with absorbers and pumps (CDR)

The whole vacuum system shall be designed with a cost-effective and sustainable approach.

New technologies in development for HEP and of interest for FCC-ee

Beyond the vacuum challenges related to the synchrotron radiation and dynamic vacuum, the vacuum system shall have an affordable cost.

Technical solutions shall be defined to minimize the cost of the system. The production should be based on series industrial processes and with a minimum of interfaces.

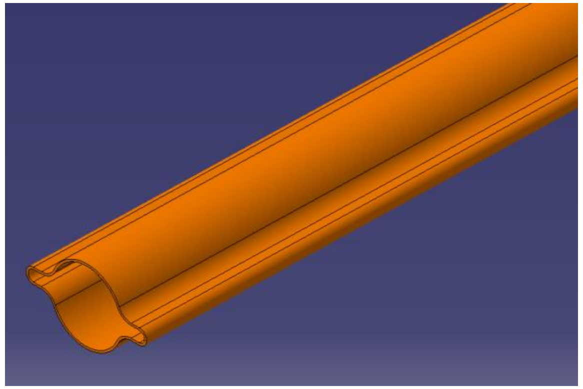

Copper extrusion

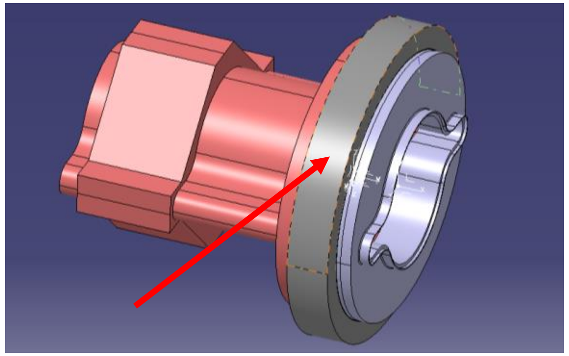

SMA connector

Some technologies are being developed and assessed for the main ring vacuum chambers:

- Shape Memory Alloy UHV connectors for:
    - Interconnection.
    - BPM pick-ups.
- Gas dynamic cold spray for:
    - Additive manufacturing of copper.
    - Permanent radiation hard bake out system.
- Weld of extruded chamber/flange.
- Local compact absorbers

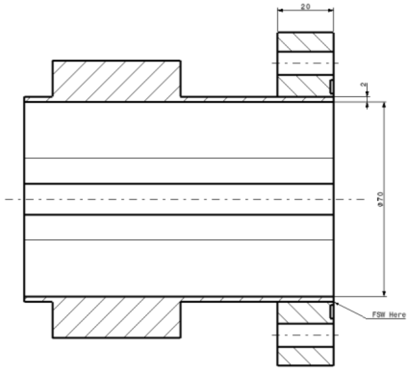

Welding extrusion/flange

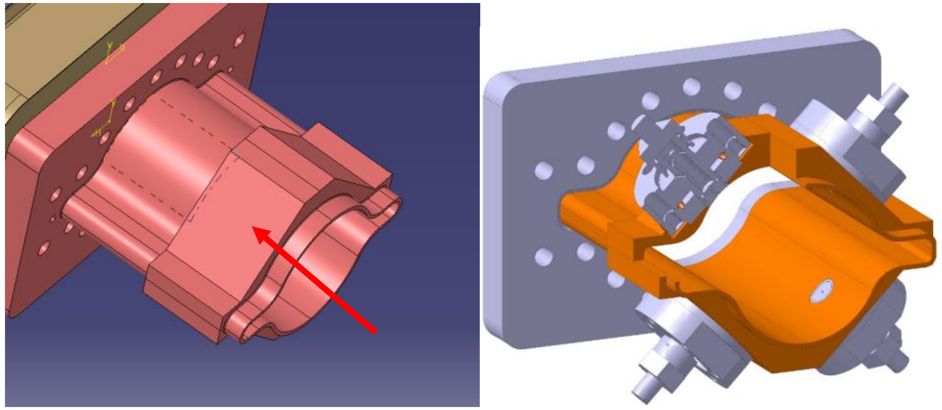

Cold sprayed copper for BPM integration

Concept of SMA connectors for UHV applications

Standard vacuum coupling systems

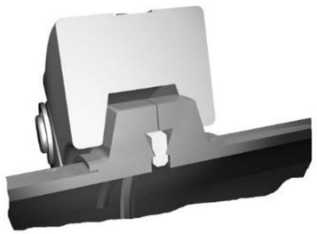

Soft/hard materials +
mechanical force

Image source: web

Shape memory alloy couplers

Austenitic contracted hot-shape

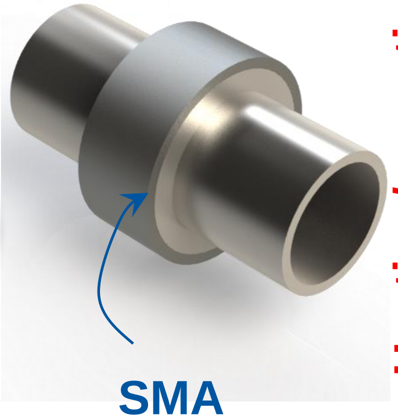

SMA ring coupler

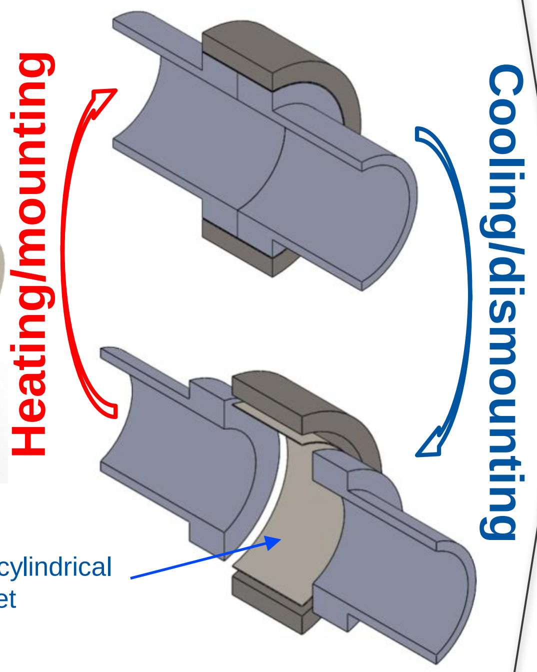

Thin cylindrical gasket

Martensitic enlarged cold-shape

Soft/hard materials + temperature control

Operation principle

- A_s: Austenite start temperature (Ring contraction starts)
- A_f: Austenite finish temperature (Ring contraction ends)
- M_s: Martensite start temperature (Ring expansion starts)
- M_f: Martensite finish temperature (Ring expansion ends)

1. Mounting at room temperature
2. Tightening by heating above 100 °C
3. Leak Rate < 10^{-10} mbar·l·s^{-1} at room temperature
4. Dismounting by cooling down to -40°C

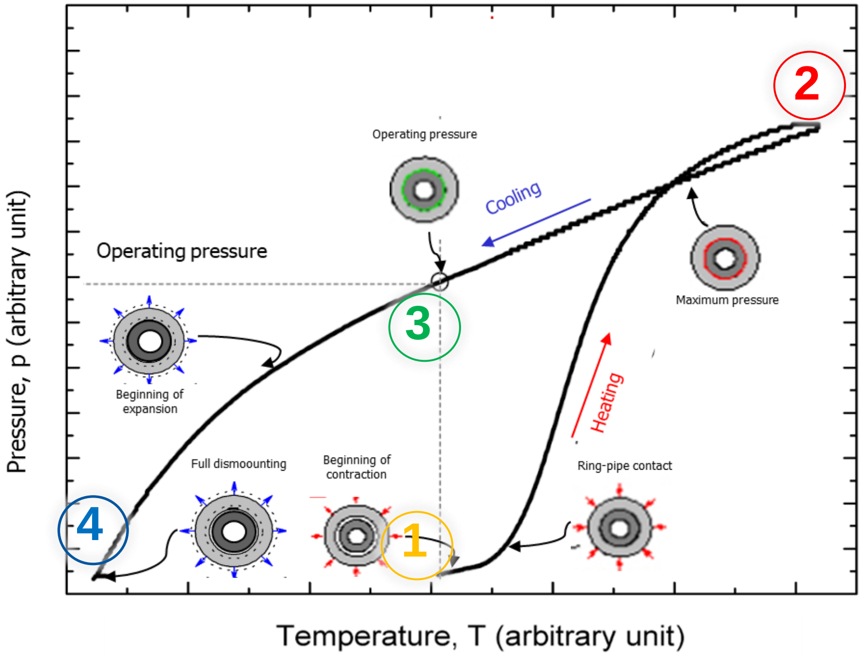

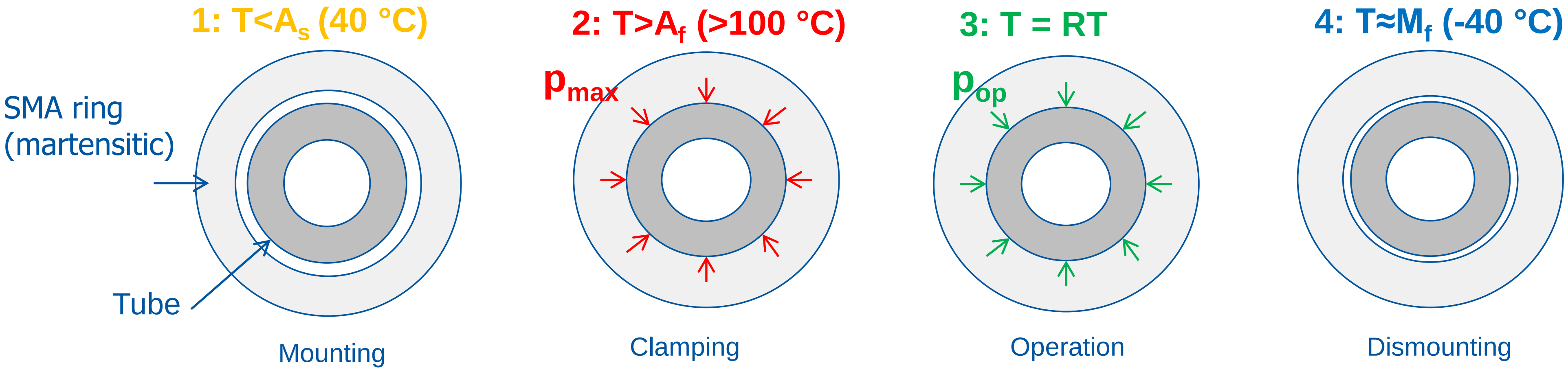

SMA-based UHV prototype joints validated

Examples of different validated SMA connectors

- Compatibility with various pipe geometries (DN16, DN25, DN50, DN100) and metals (steel, aluminum, copper, etc.)
- Bimaterial joints (St/Ti,St/Alu)
- Zero - longitudinal gap connection

Circular connectors for FCC-ee chamber/BPM button

Preliminary considerations

SMA connectors could be advantageously used to integrate the BPM pickups to the vacuum chamber :

1. More compact than DN16 CF flange.
2. Easier to assemble.
3. Transition with copper (no brazing) → cheaper.

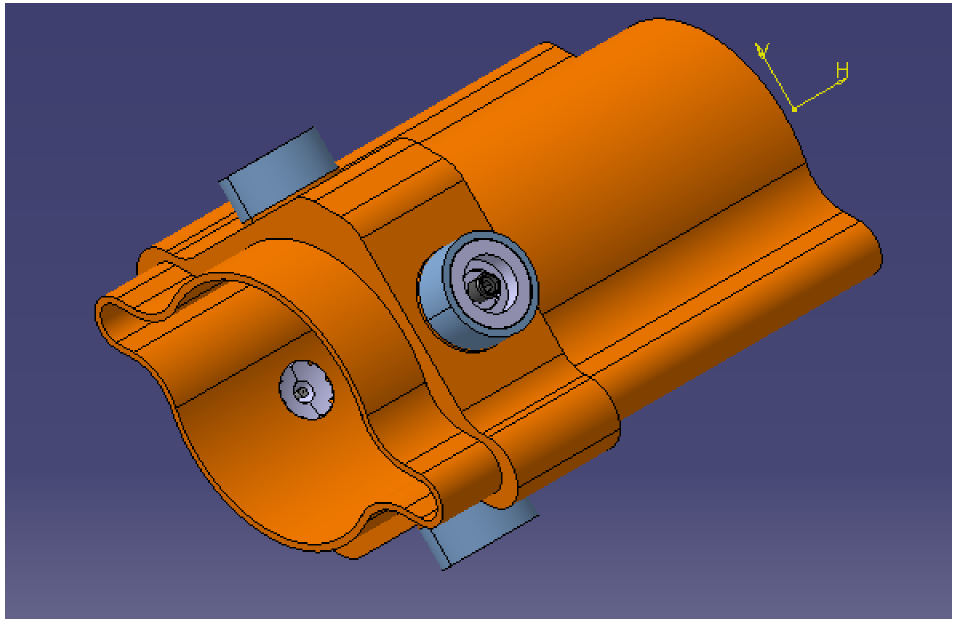

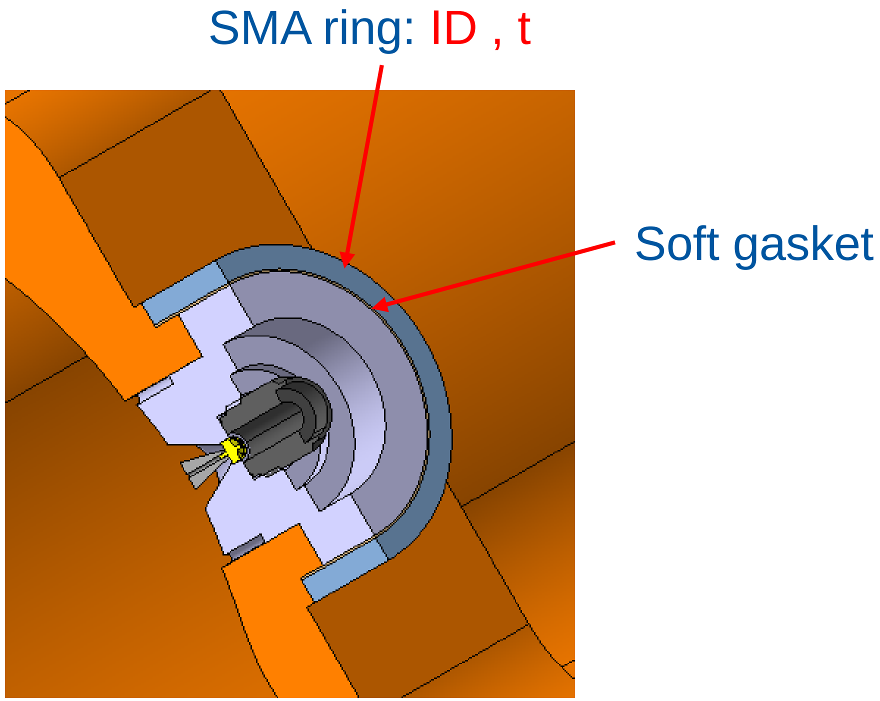

Design update of the FCC-ee BPM block on the vacuum chamber, incorporating the proposed equipment (BPM design given CERN/SY/BI for illustration)

Oval-shaped connectors for FCC-ee chamber interconnections

Preliminary analytical calculations and FE simulations

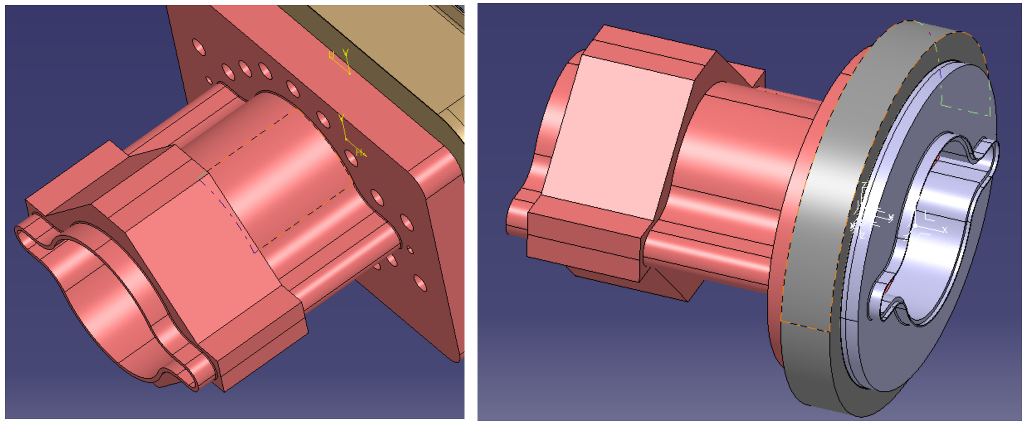

Replacement of bolted flanges by SMA connectors

Preliminary elliptic profile for SMA connector compatibility based on existing DN100 QCF.

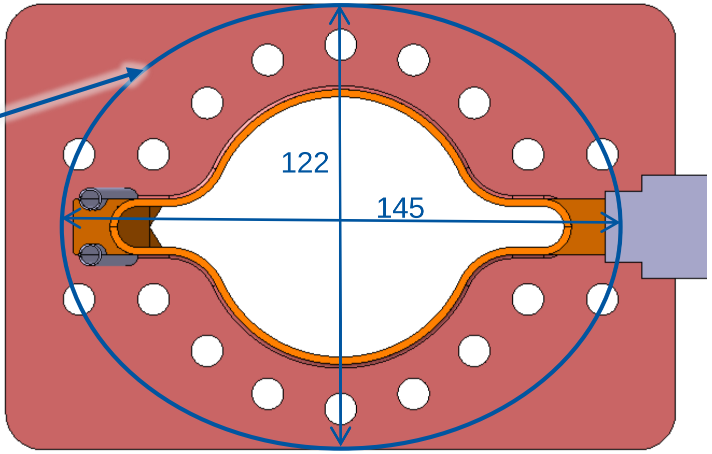

Typical expected space in the interconnection

Challenges:

- **Non Uniform contact pressure**
- **Training of Oval SMA rings**

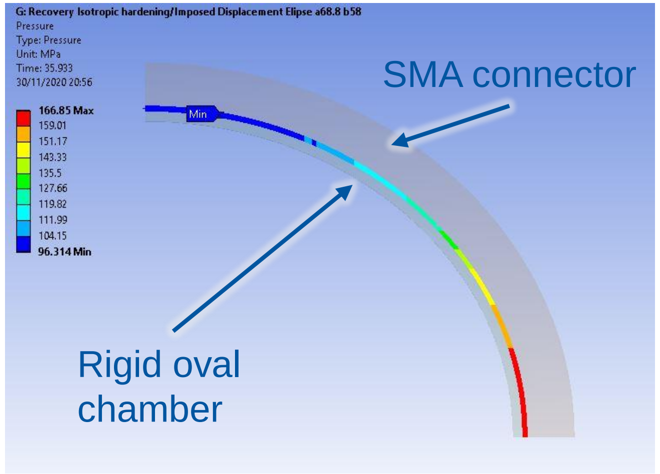

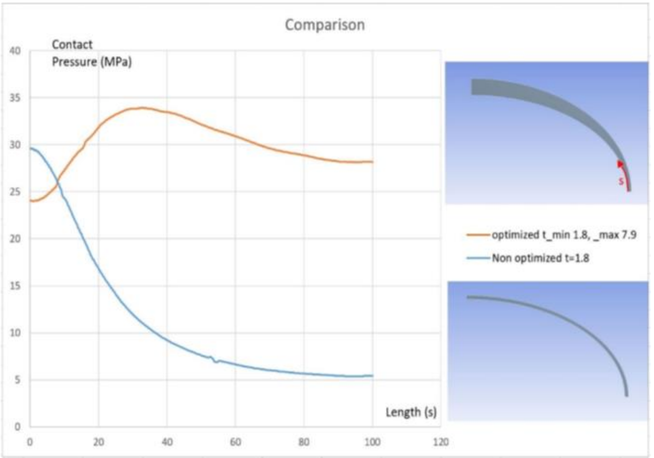

Simulations of contact pressure

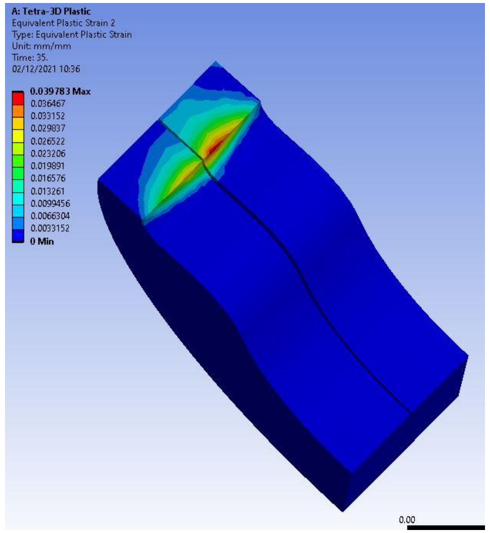

Plastic strain in the flange

Training setup for oval-shaped connectors

Design, Simulations and Manufacturing

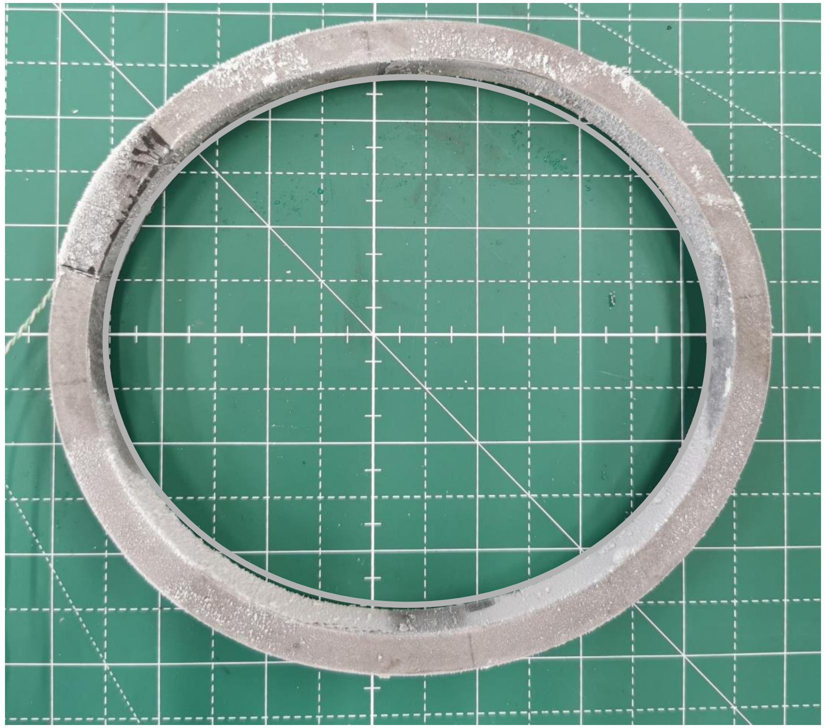

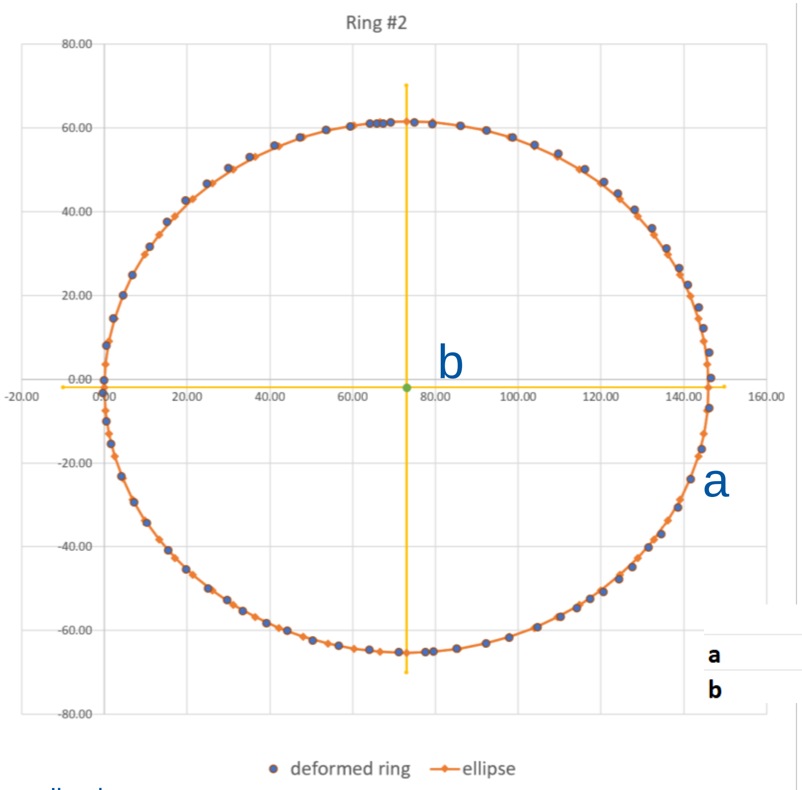

	[mm]
a	73
b	63.455

Trained ring after ovalisation

Next steps:

- Future tests
  - Recovery stress test (contact pressure measurement)
  - Repeatability of training
- Optimisation of the ring/flange and training

Principle of Cold Spray

The gas dynamic cold spray coating is based on the projection of solid powder at high velocity.

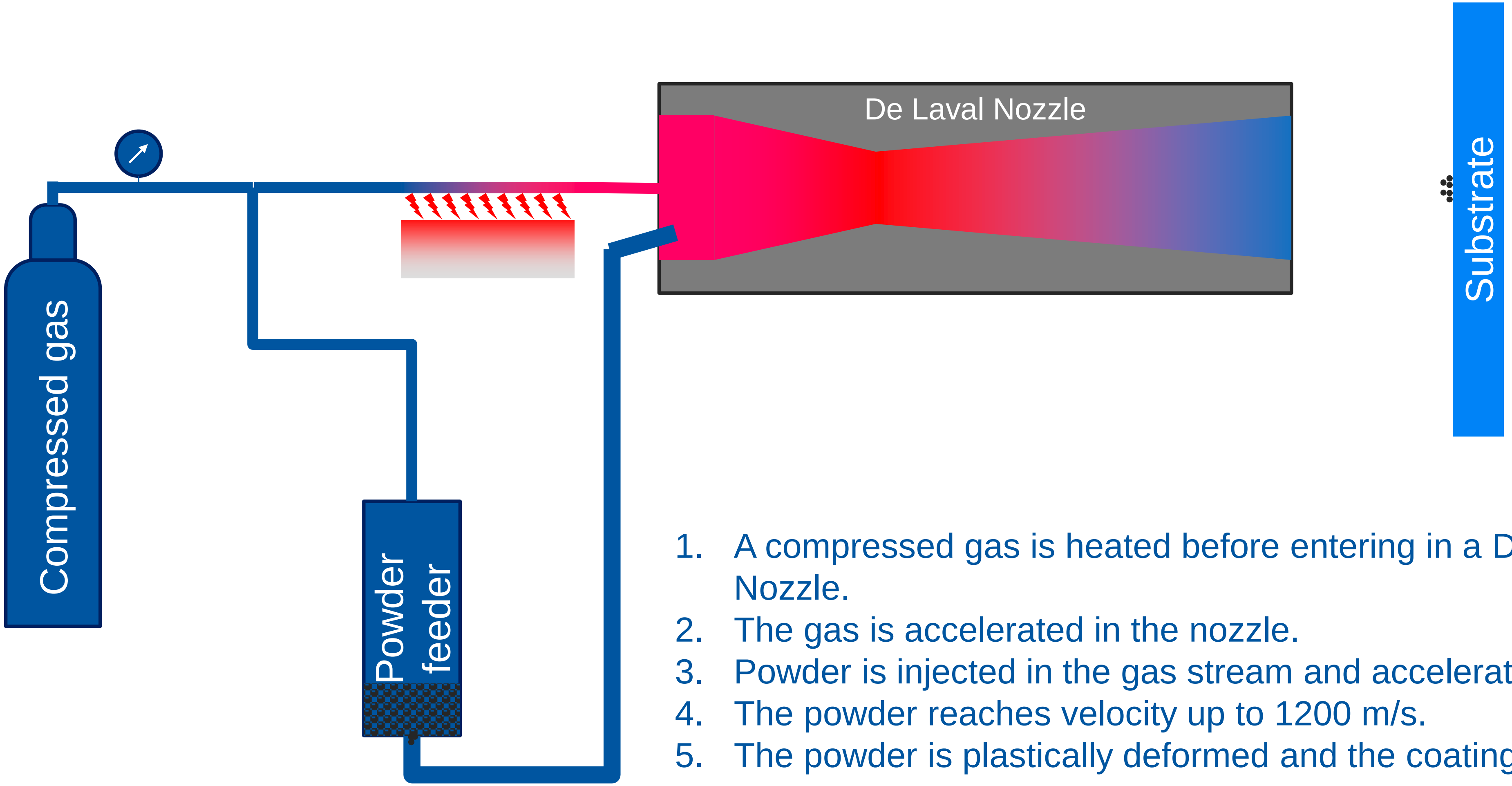

1. A compressed gas is heated before entering in a DeLaval Nozzle.
2. The gas is accelerated in the nozzle.
3. Powder is injected in the gas stream and accelerated as well.
4. The powder reaches velocity up to 1200 m/s.
5. The powder is plastically deformed and the coating is building up.

Cold Spray Advantages and Limitations

Advantages:

- No powder melting.
  - → No phase change.
  - → No grain growth.
  - → Low heating of the substrate.
- No significant impact on the oxide content w.r.t. initial material.
- Powder mixture possible.
- Compressive residual stress (fatigue life increase).
- Nozzle geometry can be tuned for a given jet size.
- Thick coating.
- High deposition rate.

Limitations:

- One constituent has to be ductile.
- Accessibility to the surface to be coated.

Possible applications:

- Additive manufacturing
- Coating (surface or local coating, metallization of polymer)
- New materials (composite material)

New Manufacturing Process

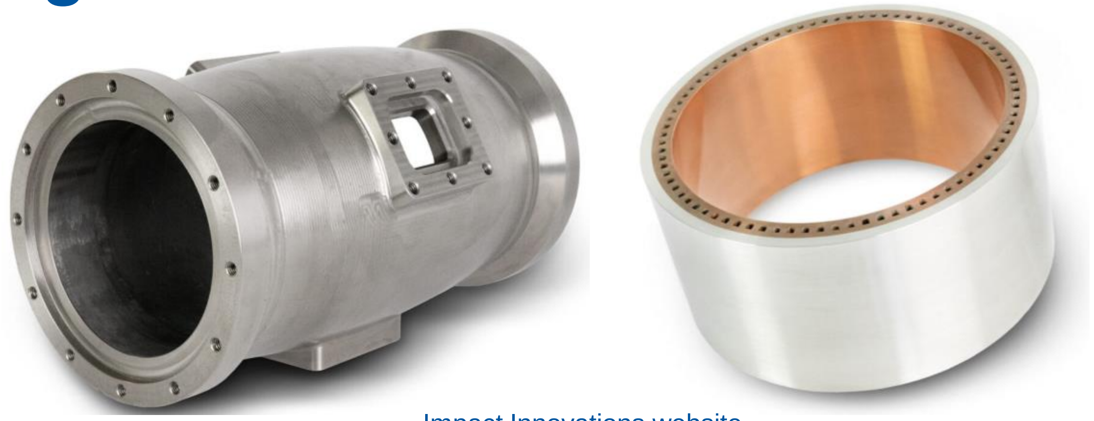

Impact Innovations website

Additive manufacturing for:
- Manufacturing of components of potentially dissimilar materials
- Joining of dissimilar materials
- New feature
- Repair
- Local reinforcement of thin walled structure

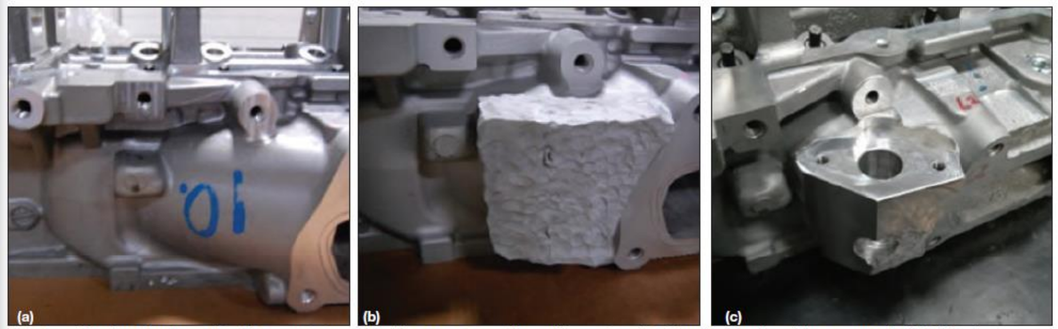

Fig. 3 — *Freeform feature added to a prototype machine component by cold spraying. (a) Prior to spraying, (b) as sprayed, (c) finished.*

J. Villafuerte, ADVANCED MATERIALS & PROCESSES, 2014

Cold-Spray utility in FCC-ee: new feature

Conceptual design for Beam Position Monitor integration on the vacuum chamber.

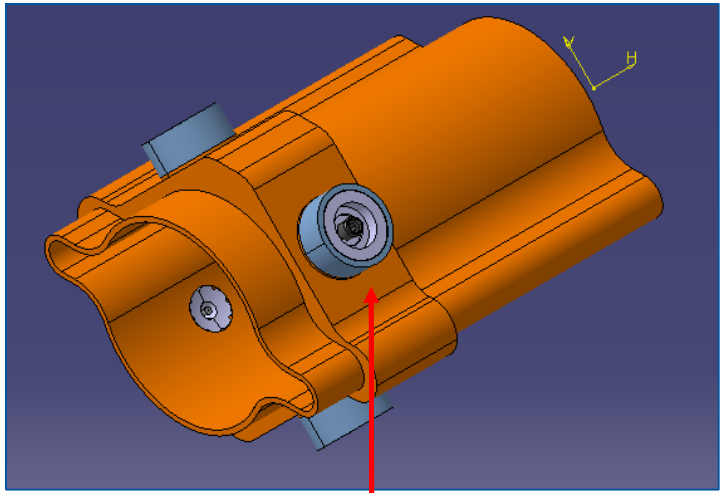

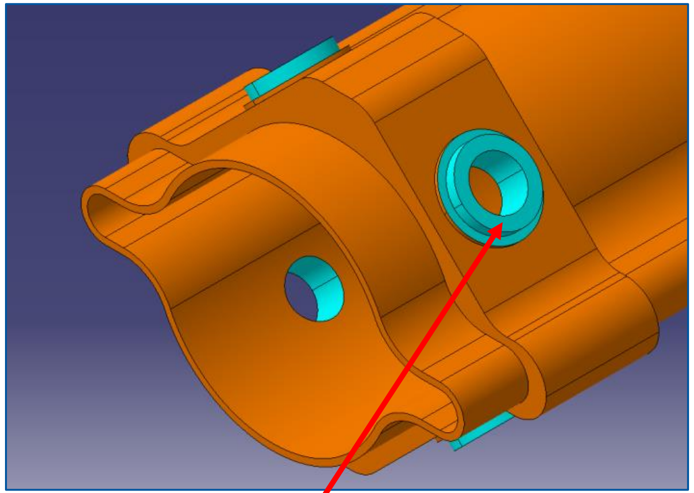

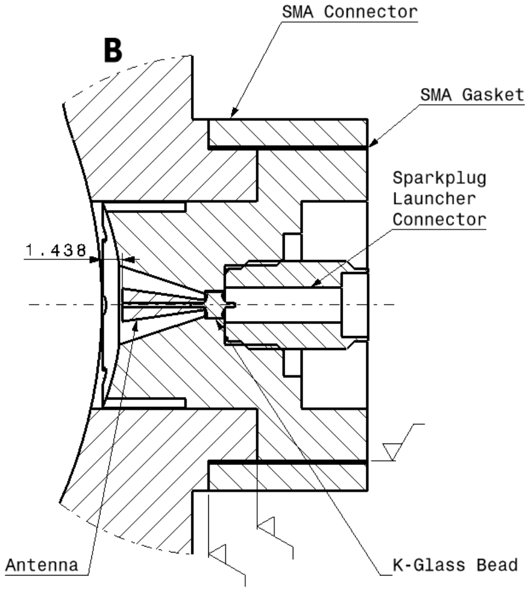

Cold sprayed copper BPM Block onto the vacuum chamber extrusion:

- No structural interruption (no welded transition with the chamber)
- Minimum raw material
- Minimum machining

Machined (Blue) boss to support BPM components

BPM Components mounted on the machined boss.

Shape Memory Alloy (SMA) gasket and connector used to secure the flange to the boss and ensure the leak tightness.

Interface for positioning of the BPM in the QUAD can be done in the same way.

Suitability of cold spray additive manufacturing for UHV applications?

Leak tightness of cold sprayed additive materials:

A previous study on aluminium coating has shown [1]:

1. Helium leak tight coatings are achievable.
2. The presence and the role of microporosities formed during the process.
3. The influence of powder morphology on the porosity formation.

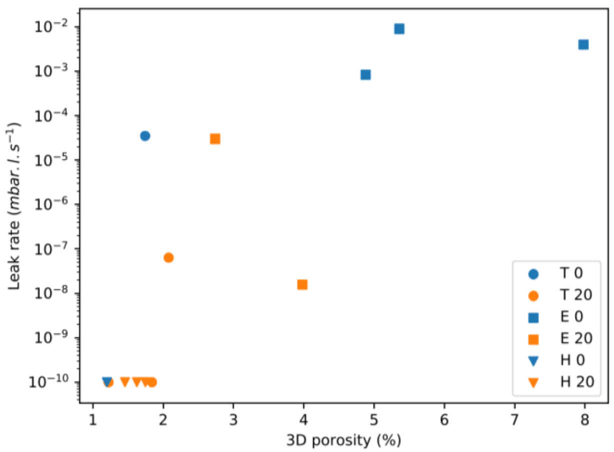

Influence of porosity on leak tightness for different powders and process parameters [1]

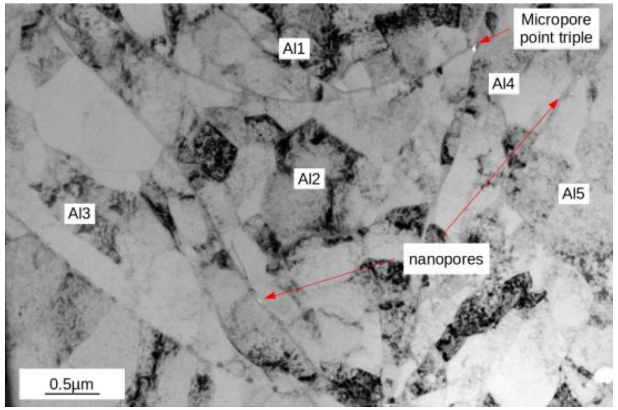

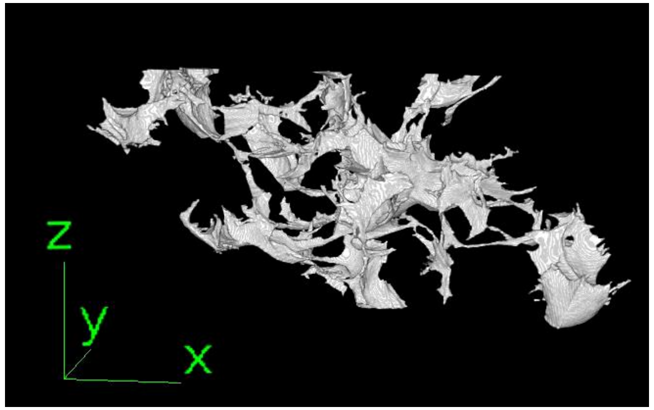

Porosity formation in cold sprayed aluminium [1]

[1] Etude de la relation entre porosité et étanchéité à l'ultra-vide de dépôts à base d'aluminium obtenus par projection dynamique par gaz froid ("cold spray"), Sébastien Weiller: http://www.theses.fr/2021UPSLM004

Cold-Spray UHV Validation – leak tightness

Samples, with different alumina contents, have been produced to test the leak tightness under different configurations:

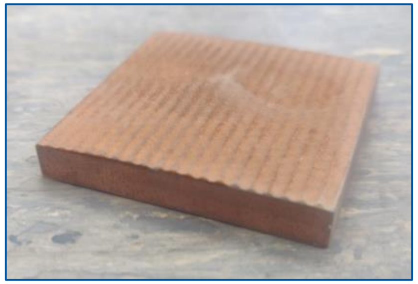
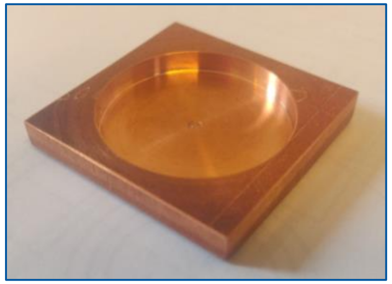
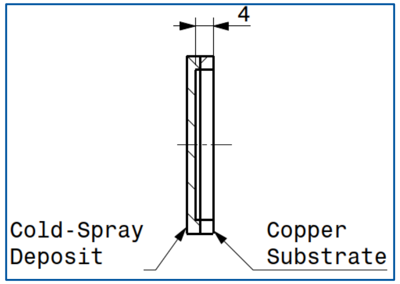

Cold-Spray sample used for leak tightness

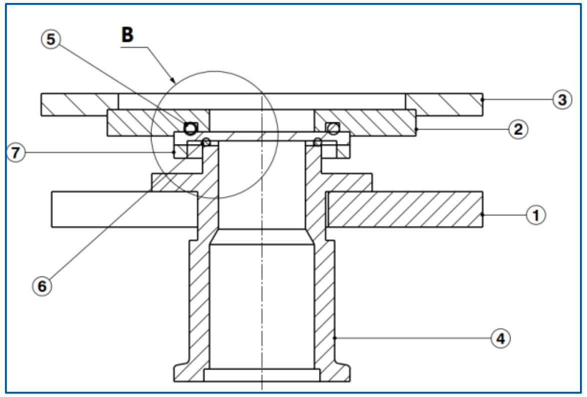

Variant to test only the Cold-Spray deposit

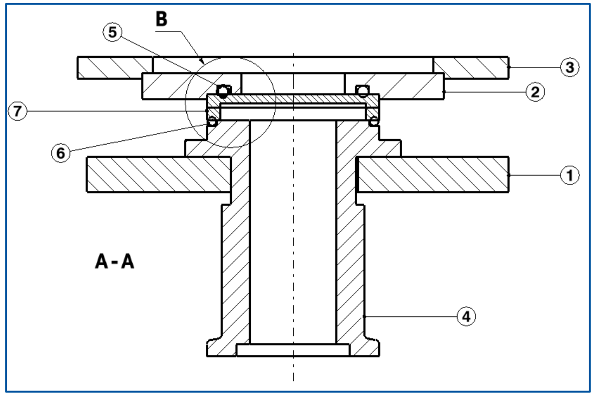

Variant to test the deposit and the interface to the substrate

The tool is clamped to the detector and all samples were tested.

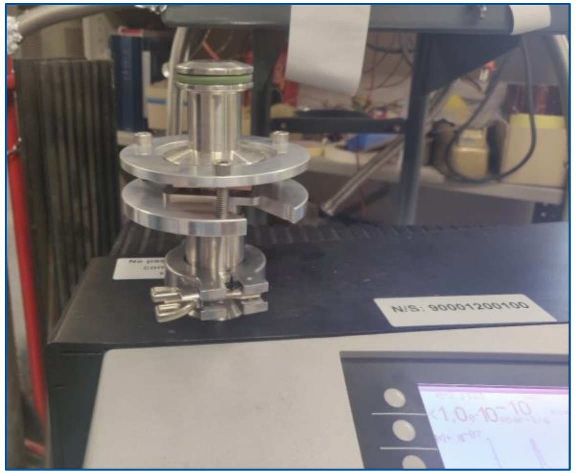

All samples passed.

All samples subjected to thermal cyclical shock testing – no issues reported.

Further tests ongoing to find the minimum thickness of deposit to maintain leak tightness.

Cold-Spray UHV Validation – thermal outgassing

Thermal outgassing measurement is based on gas accumulation across different time intervals. Predominantly concerned with hydrogen.

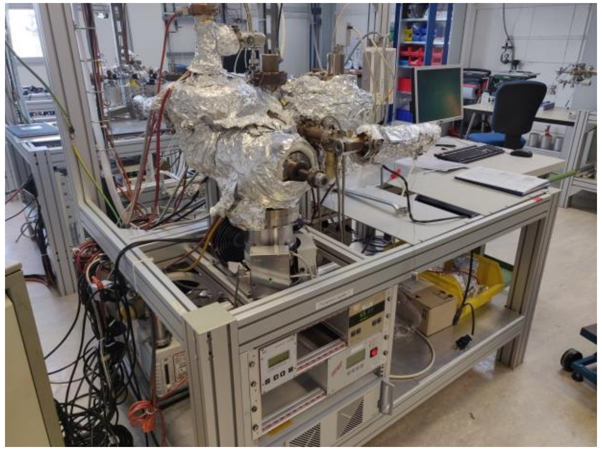

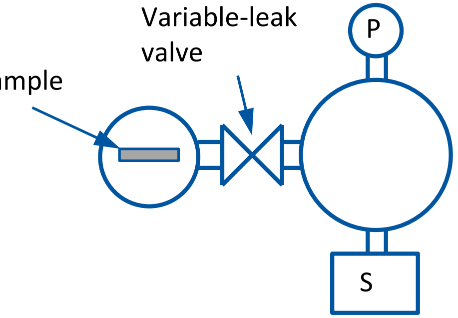

Test bench for thermal outgassing measurement by accumulation of baked samples

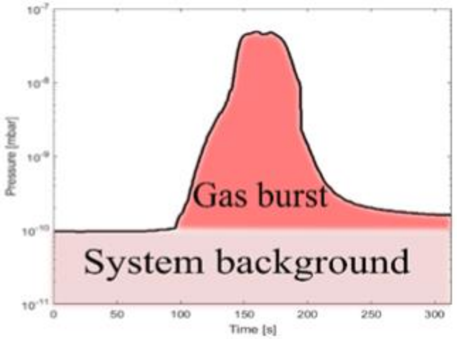

Typical pressure curve

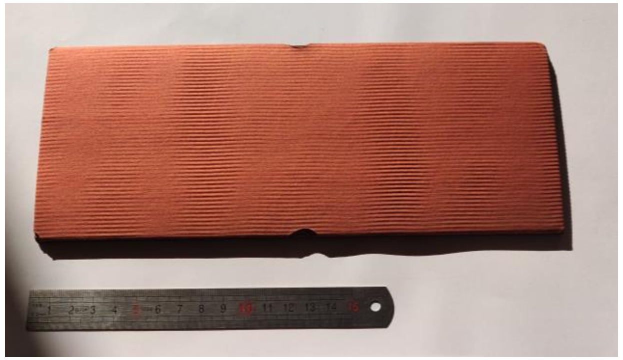

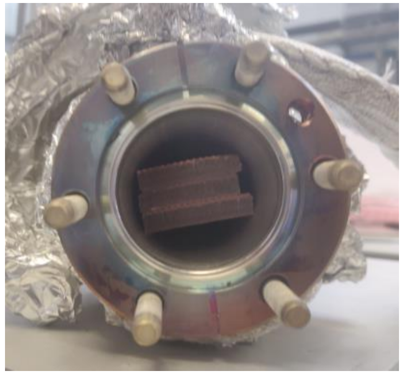

Cold-Spray samples placed into chamber,

Set-up has been refurbished, commissioned and is ready for the thermal outgassing measurements of the cold spray samples.

Cold-Spray UHV Validation – Metallography

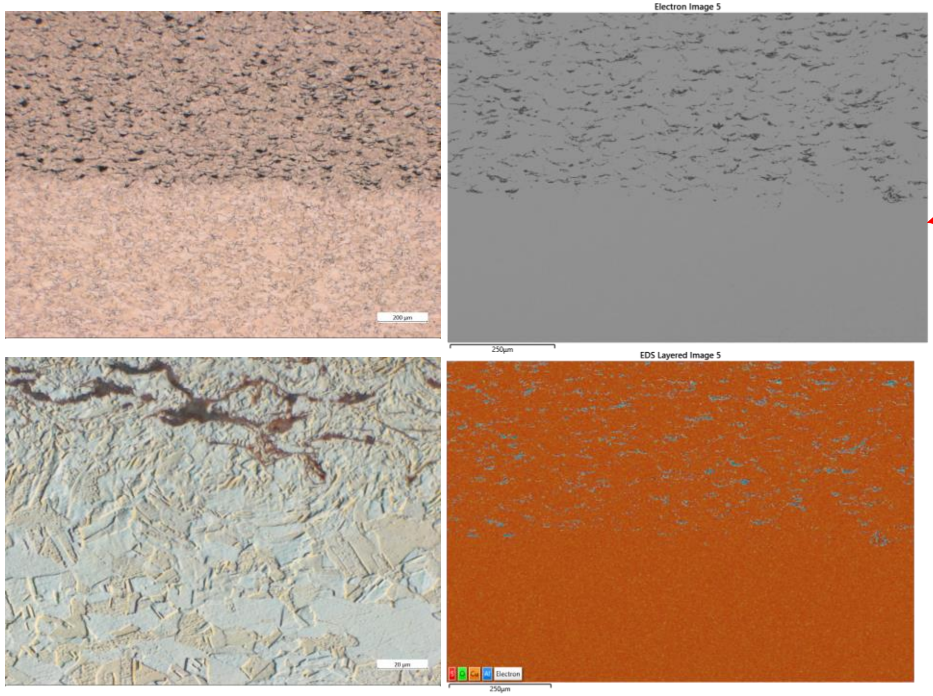

Optical and SEM-EDS analyses of the interface between cold-sprayed layer and OFE copper substrate (70/30 sample)

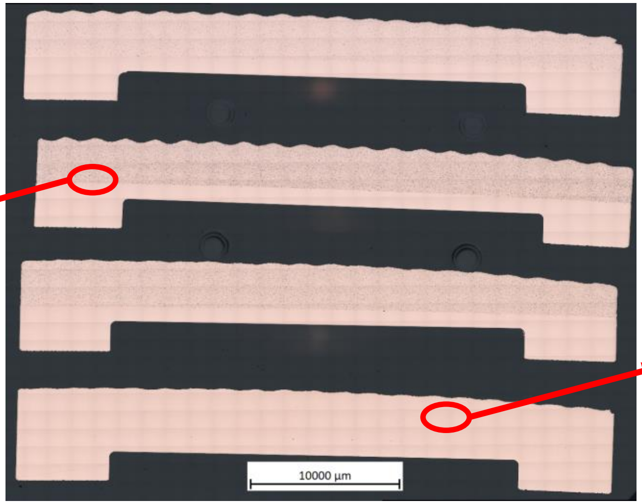

Samples of OF copper with 0, 10, 20 and 30% of alumina deposits on OFE substrate

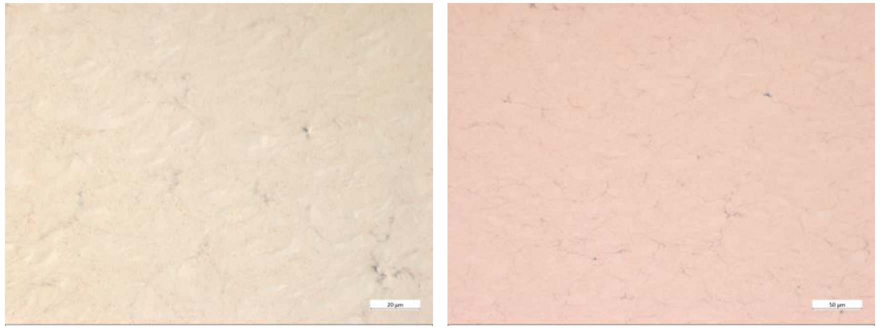

100% OF copper as-polished Fine network of oxides is visible (light grey points)

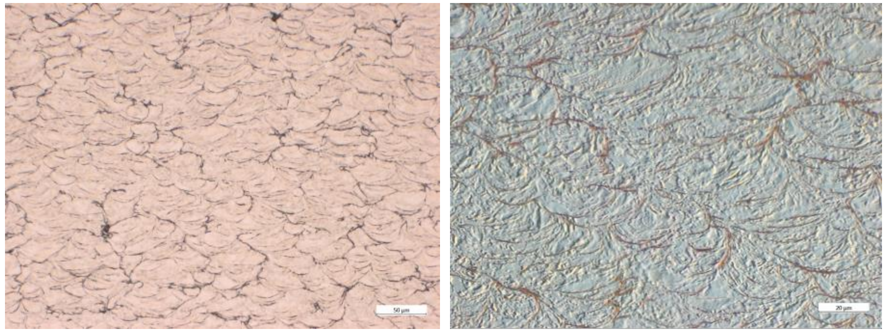

100% cold sprayed OF copper material as polished and after etching

Observations [1]:

- Formed layers exhibit fine and homogeneous microstructures.
- For samples with alumina, Al_2O_3 particles appear homogeneously spread through the microstructure.
- Interfaces between cold-sprayed layer and OFE copper substrate appear free from imperfections such as cavities, cracks, or lack of adhesion.
- SEM-EDS examinations confirmed the homogeneity of the structures and the absence of imperfections at interfaces.

[1] FCCee - copper cold spray tests, M. Crouvizier, EDMS 2797402

Cold-Spray utility in FCC-ee: local coating

Local coating used as permanent radiation hard heating element for bake out (in or outside vacuum)

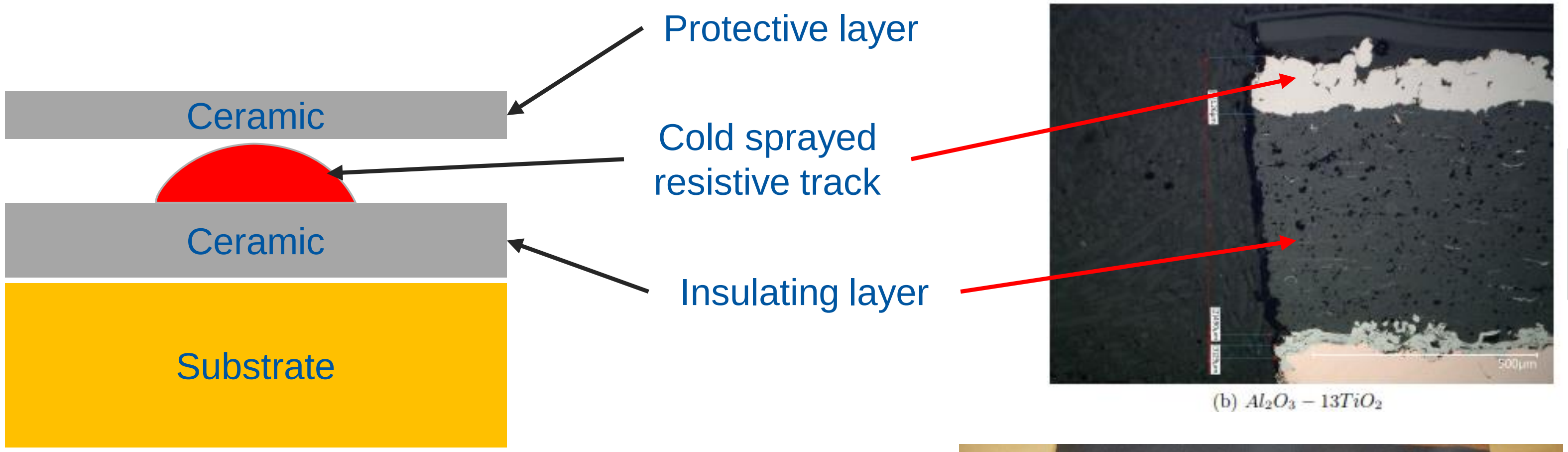

(b) $Al_2O_3 - 13TiO_2$

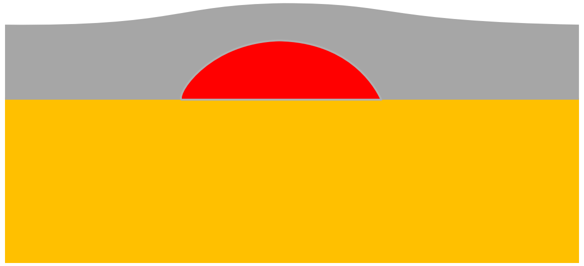

Layer Reference (Order of application)	Layer Material	Layer Thickness (mm)
01 - Substrate	Cu OFE C10100	2
02 - Bond-coat	Nickel, Aluminium	0.05
03 - Underlayer	Ceramic Al(2)O(3) – 13T iO(2)	0.5
04 - Track	Titanium Grade 2	0.2
05 - Insulation	Ceramic Al(2)O(3) – 13T iO(2)	0.1 - 0.2

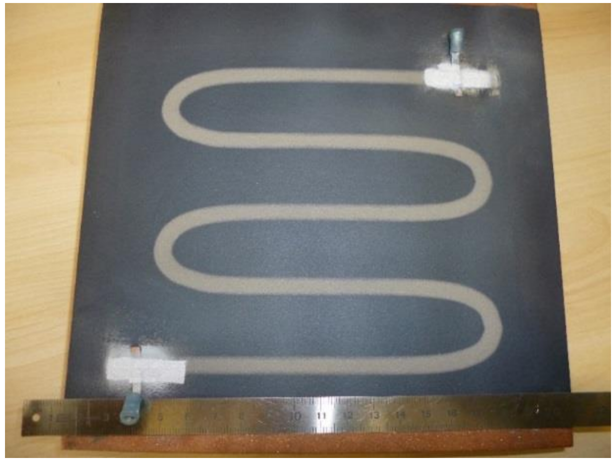

Copper plate with plasma sprayed ceramic and 0.2 mm thick cold sprayed titanium heating track

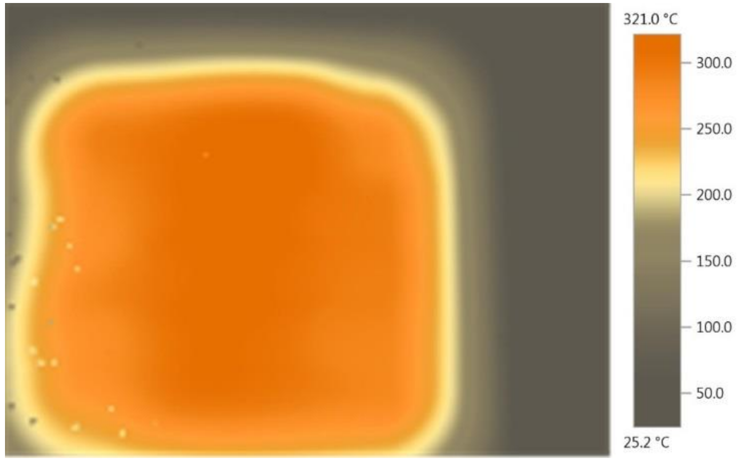

Measurement of the temperature field

Cold-Spray utility in FCC-ee: local coating

Integrated, permanent radiation hard bake-out track for vacuum chambers. First design S-Type Track.

- Spatially compact design
- Homogenous temperature distribution

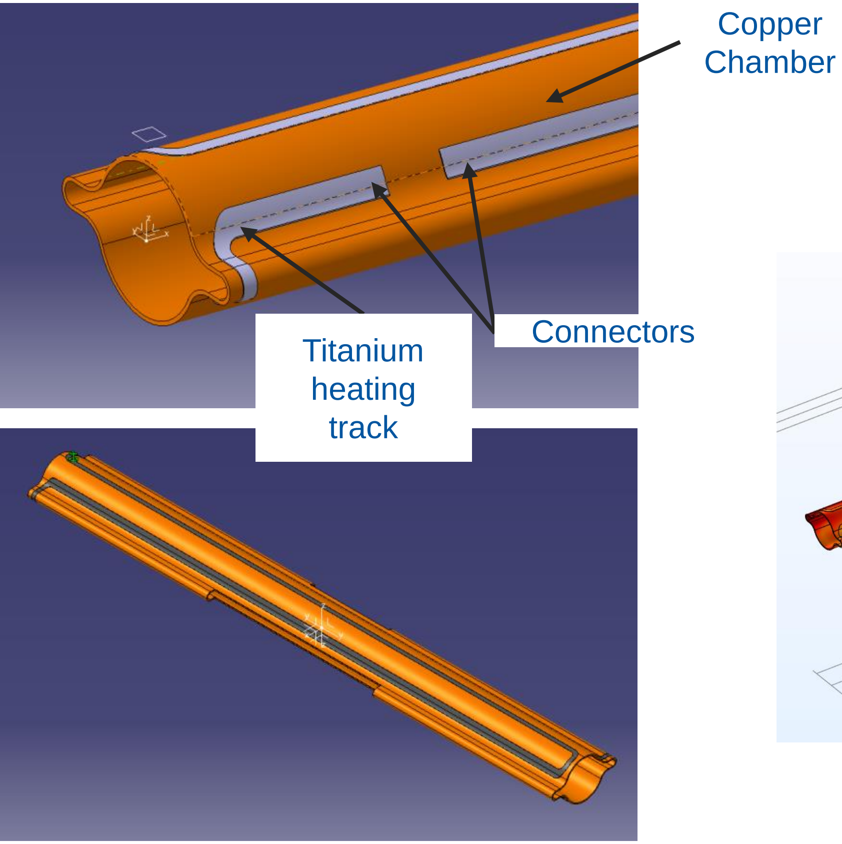

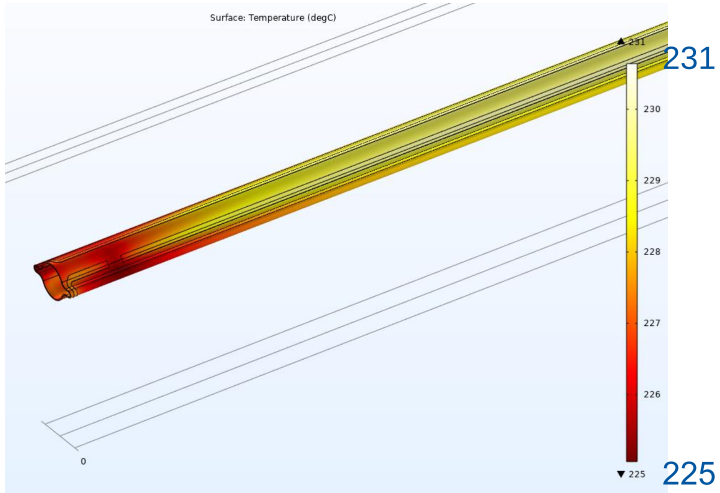

Expected temperature field along the vacuum chamber

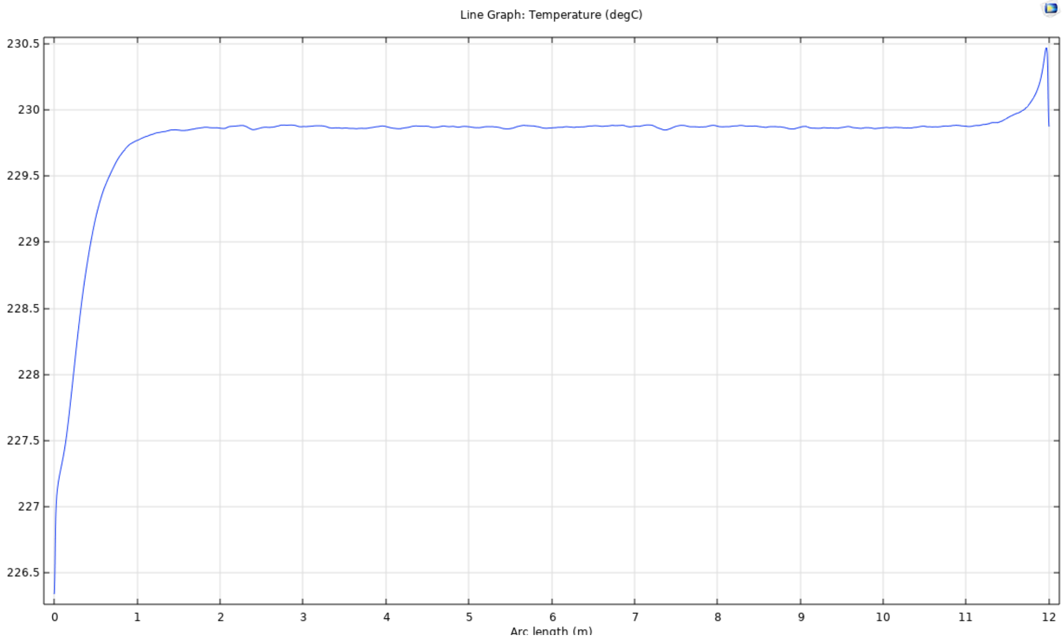

Expected temperature profile along the vacuum chamber

Cold-Spray local coating – Proof of concept

A first prototype of a copper tube with a permanent radiation tolerant bake out system has been produced:

- OFE copper tube, 84 mm * 2 mm, 500 mm long
- Al_2O_3-TiO_2 ceramic layer
- Track in titanium, ~ 110 μm thick, 8 mm width
- Distance between the tracks: ~30 mm

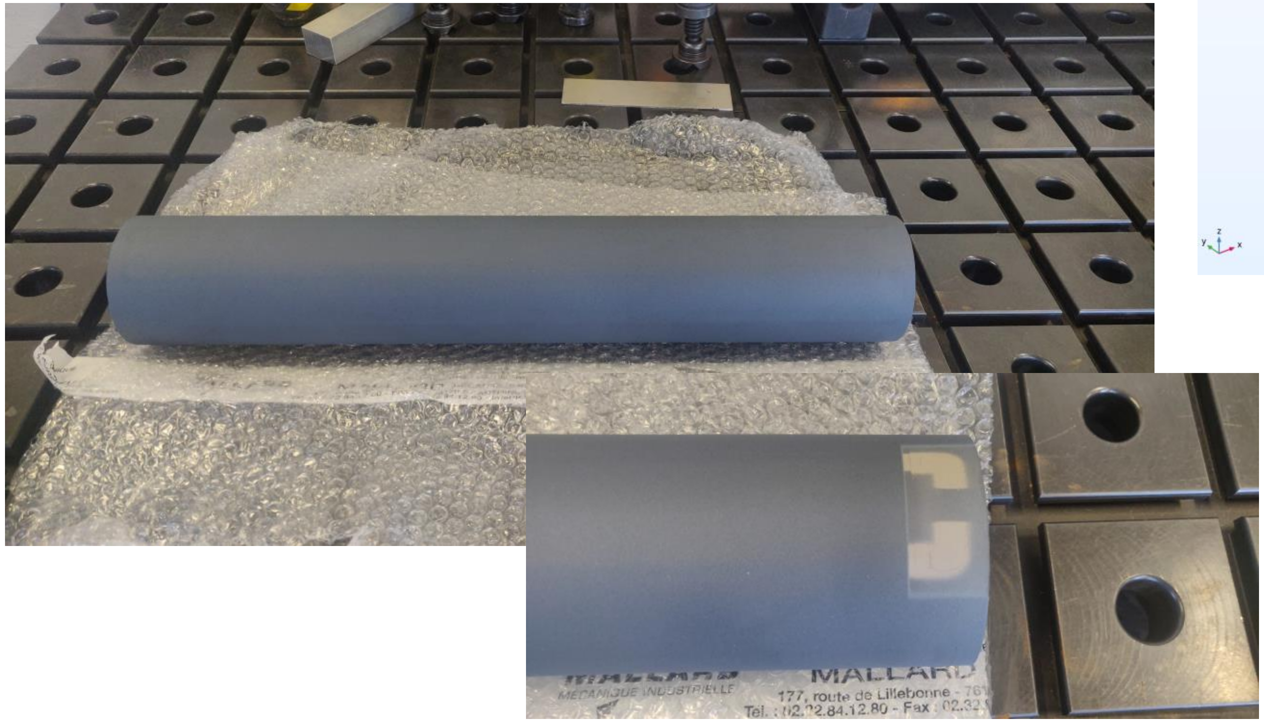

Interfaces for the electrical connections

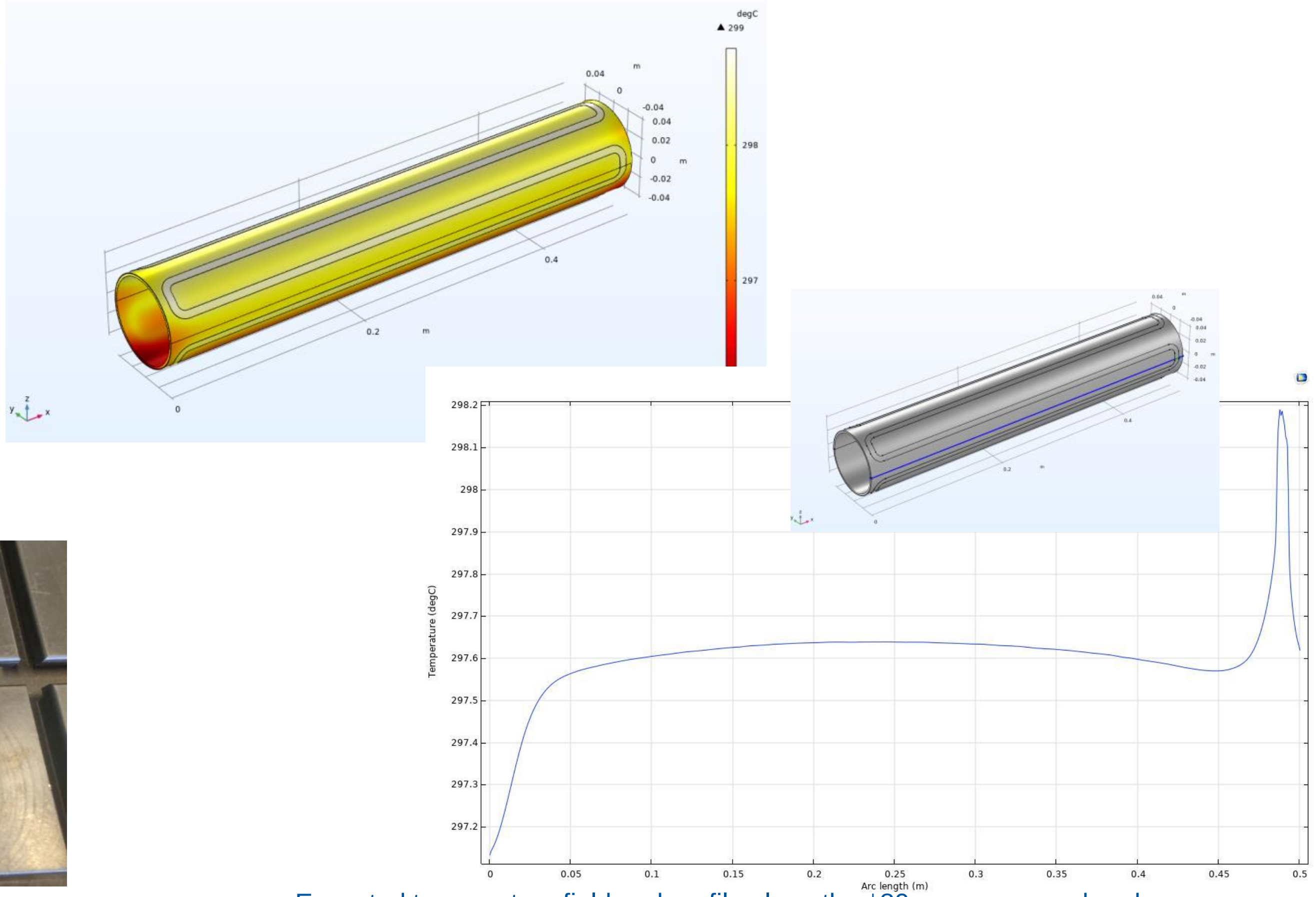

Expected temperature field and profile along the ϕ80 mm vacuum chamber prototype

Cold-Spray local coating – Proof of concept

Thermal tests:
- Low thermal conductance supports
- DC current power supply
- Electrical connections clamped on the tube

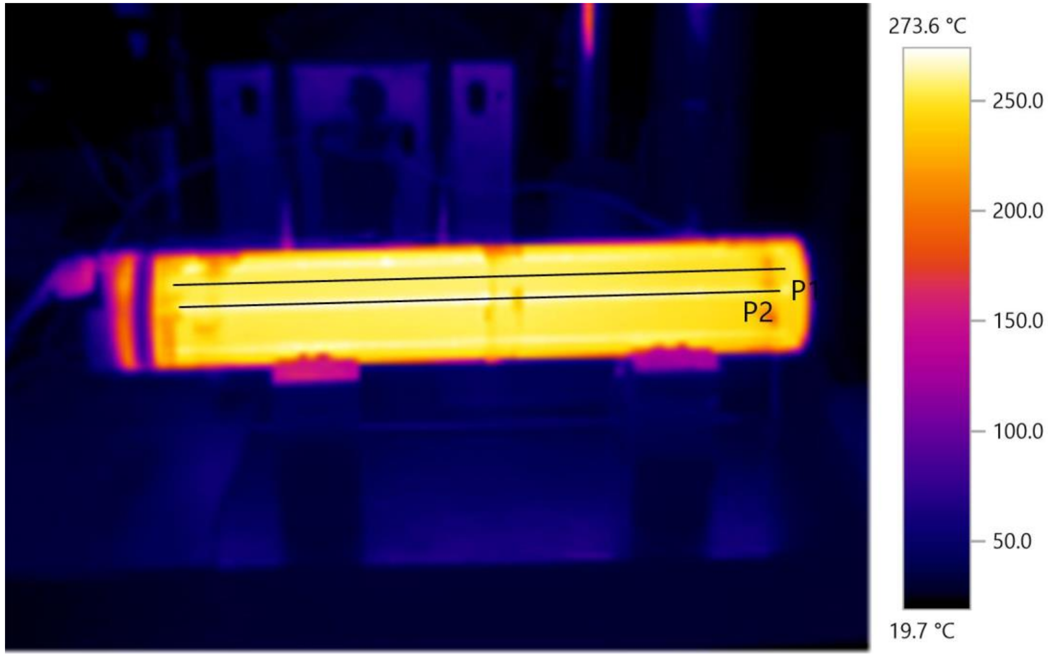

Temperature field

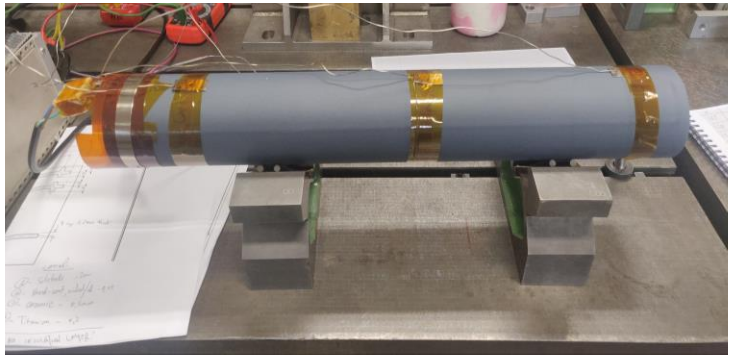

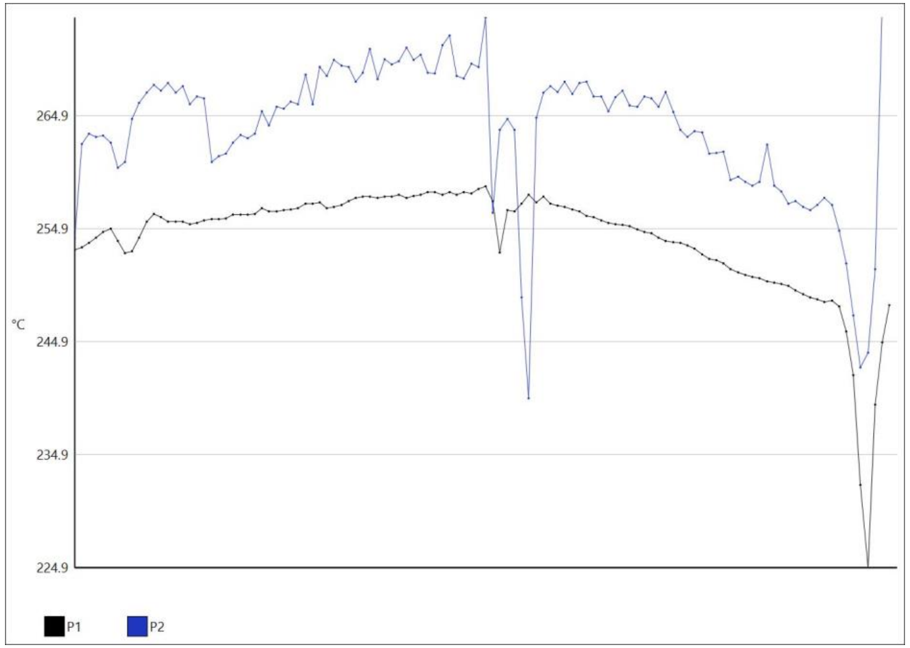

Longitudinal temperature profile

- ➢ Successful heating to more than 250 °C.
- ➢ Good temperature homogeneity: +/- 10 °C.

Synchrotron Radiation Absorber (SRA)

SR is a significant source of heating and photoelectrons, as such, absorbers are required. In order to not affect impedance, the winglets ‘capture’ the SR.

These will be installed every ~5.6m in the dipole chambers to intercept the SR.

Need to intercept between 4 and 7 kW of power depending on the location along the arc lattice.

Oblique surface ~300mm long.

Material: CuCrZr.

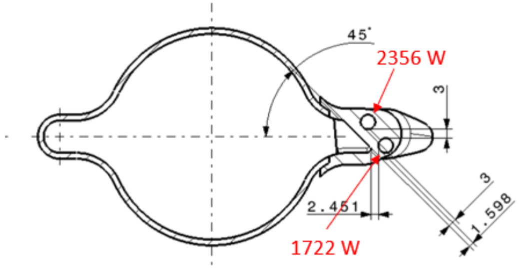

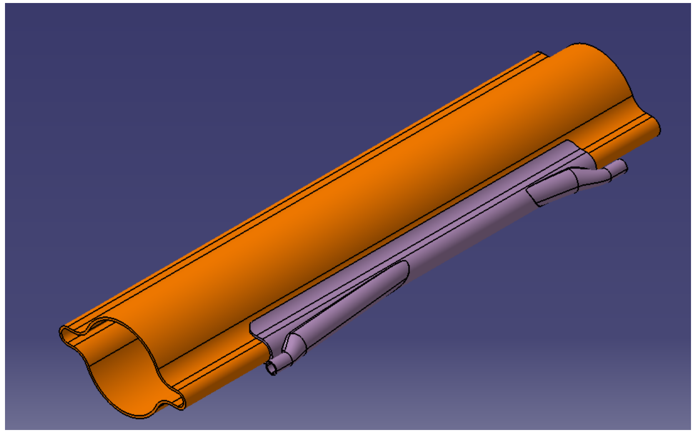

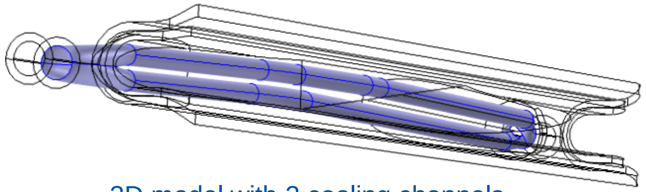

3D model with 2 cooling channels

Ease of manufacturing:

Complex geometry, internal spiral (heat transfer enhancement).

Selective Laser Melting (SLM) additive manufacturing has been selected to manufacture the first prototypes.

Other samples using SLM are being procured for various qualification tests at CERN (Tensile, porosity, density, leak tightness, etc).

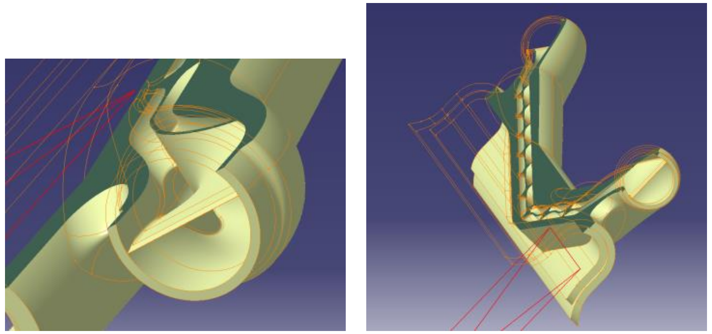

Twisted tape to increase the heat convection coefficient

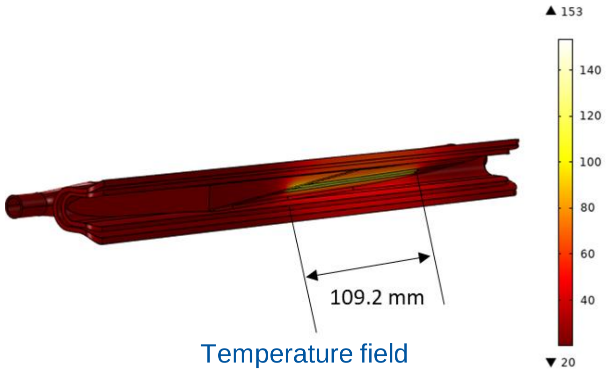

Temperature field

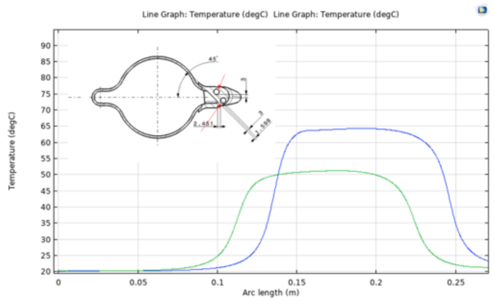

Temperature evolution along exchange surface

Flange connection by Friction Stir Welding (FSW)

For FCC-ee interconnections, FSW is being assessed to join the flanges to the vacuum chamber in a cost-efficient manner:

- Solid state joining process.
- Mitigates many defects (porosity, crack, deformation,..) regarding melting and solidification in fusion welding.
- Automated, repeatable.
- no edge preparation.
- post-processing on same machine.

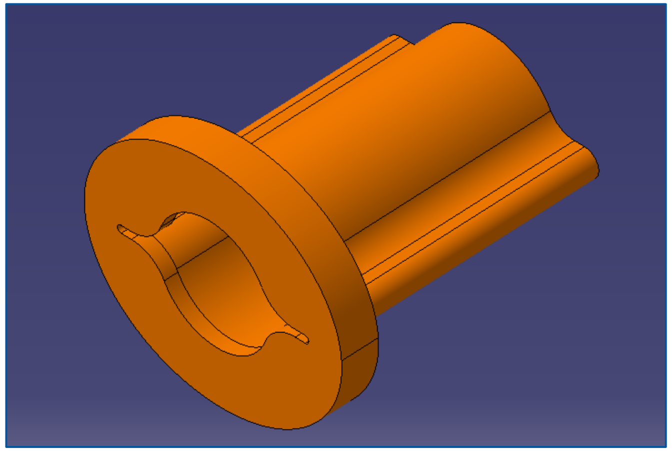

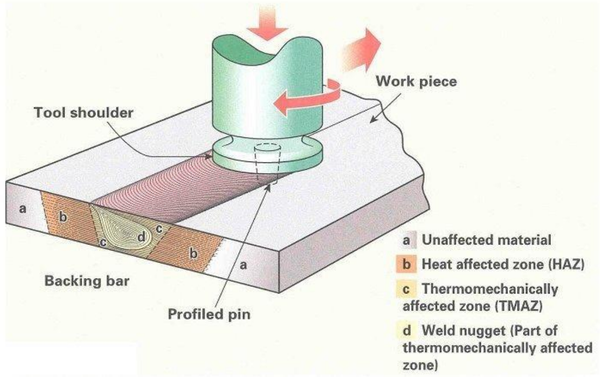

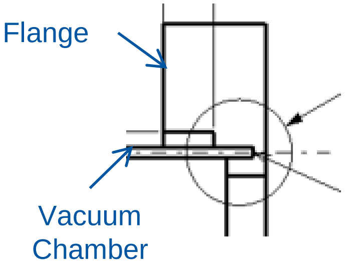

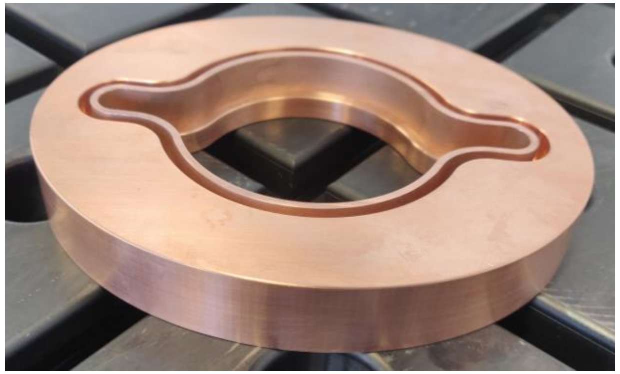

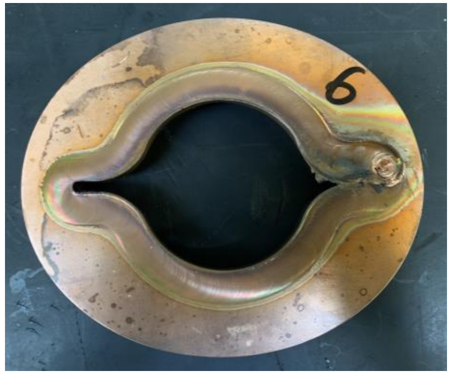

Phase 1 – destructive testing to determine optimal weld parameters, including clamp and tooling design.
Phase 1 complete, report from sub-contractor. Improvements to pre-weld flange design can be implemented

Phase 2 – joining of longer vacuum chambers (150mm) to qualify FSW for Ultra High Vacuum and for use in vacuum chamber prototype.

Interconnection conceptual design (1)

Two designs for the interconnection undergoing analysis

1. Honey-comb type fingers

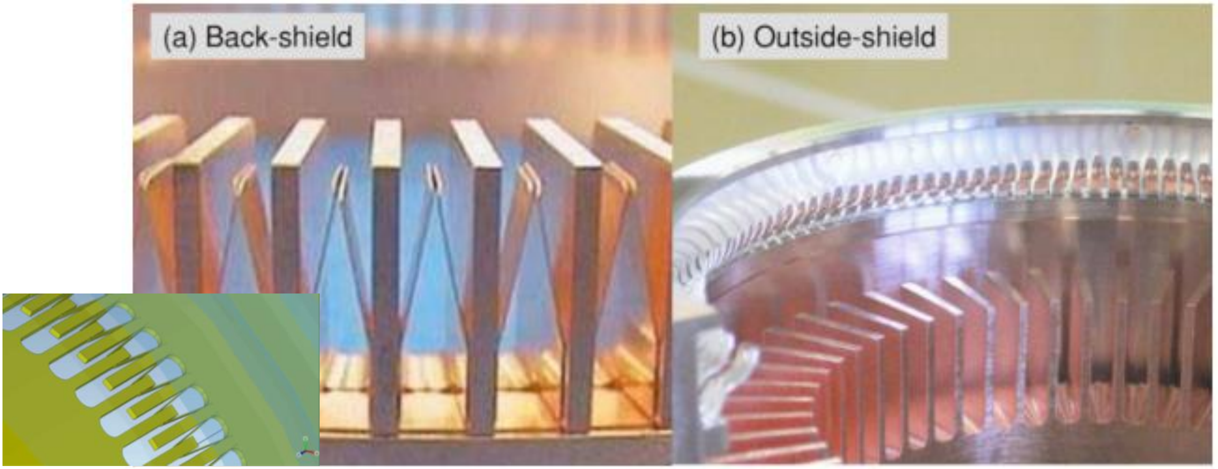

SuperKEKB ‘honey-comb’ RF ringers

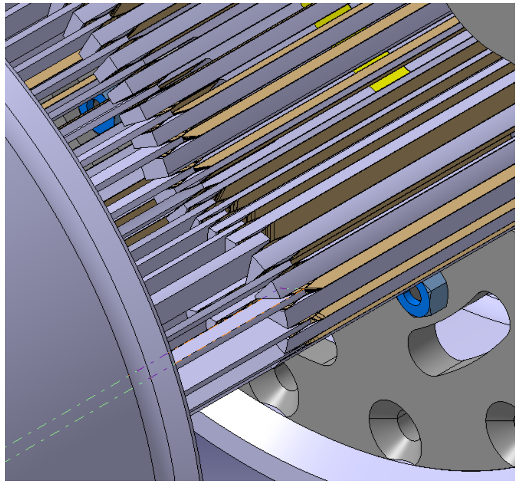

Adaptation to FCC-ee

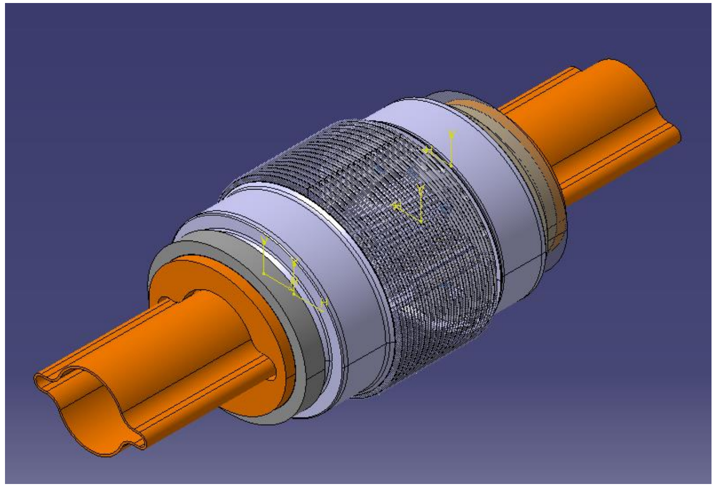

Interconnection design, showing associated bellows and flanges

Advantages:

- Tests well in Impedance testing, contributing to beam stability
- Proven design with SuperKEKB
- Maintains geometric cross-section throughout the interconnection (in absence of misalignment)

Disadvantages:

- Limited lateral misalignment and axial capability
- Likely expensive to manufacture due to fine tolerances required and complex geometry

Interconnection conceptual design (2)

Two designs for the interconnection undergoing analysis

2. Deformable RF bridge

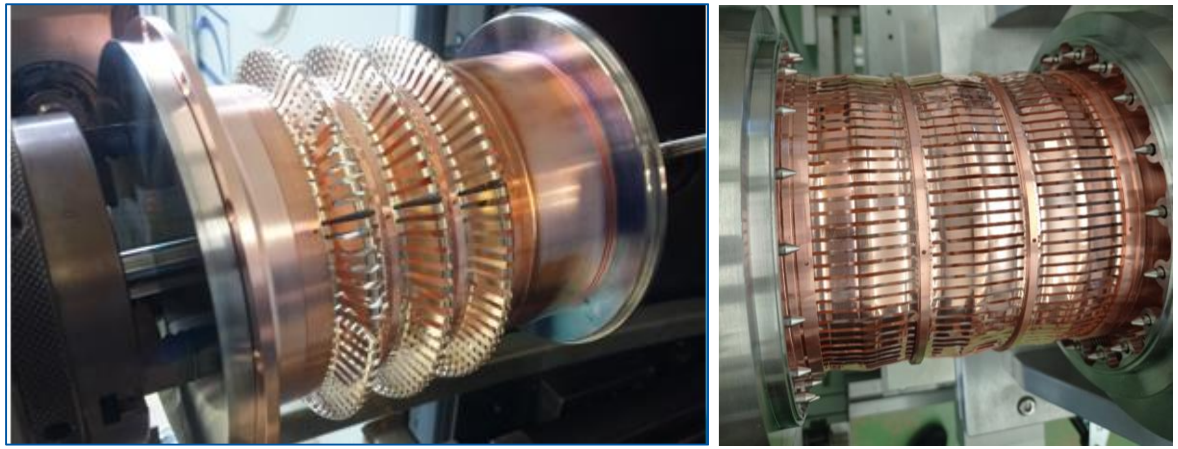

Existing connections with ‘Deformable RF’ bridge, in free and operation position

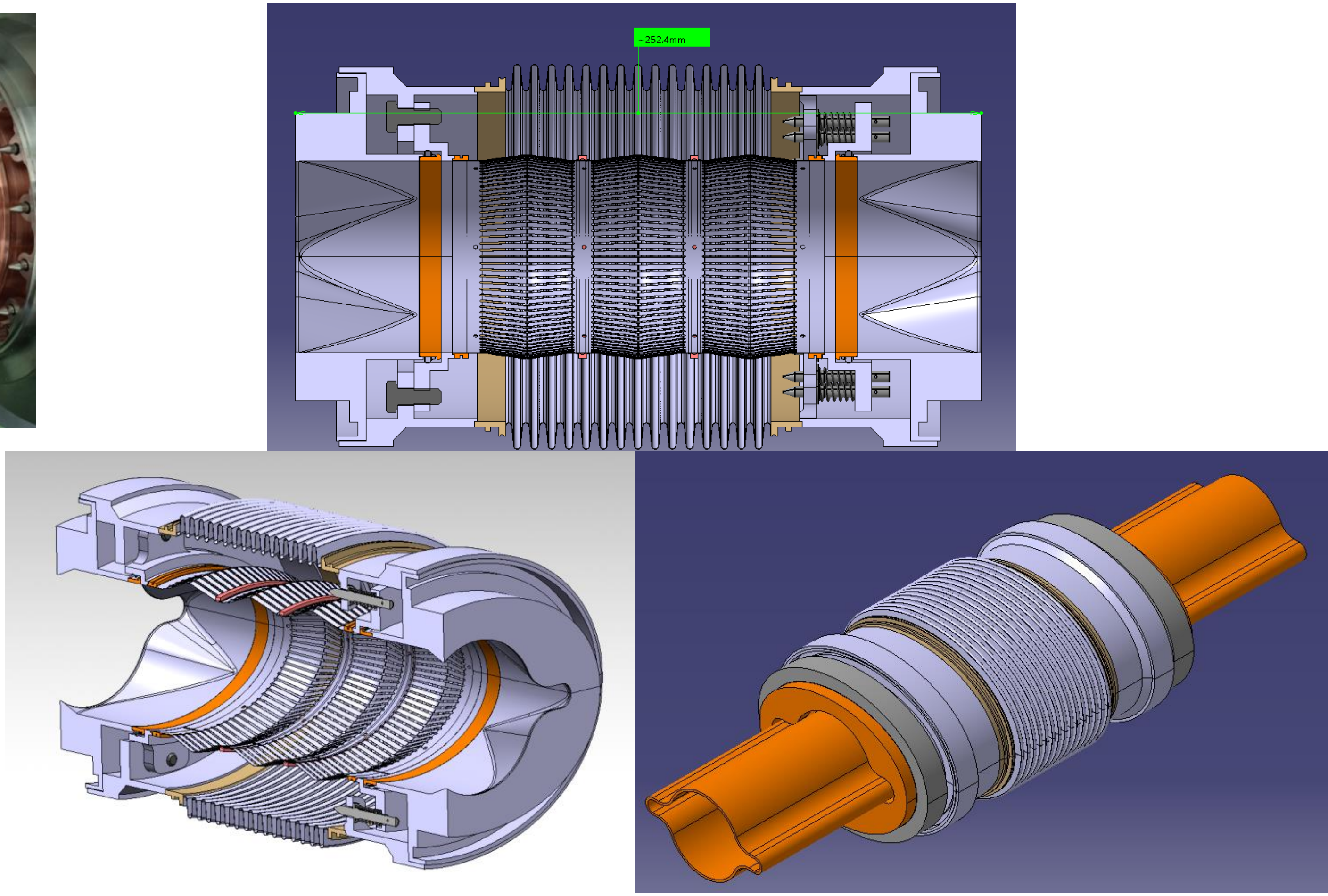

Interconnection cross-section with DRF

Advantages:

- Proven design for interconnections
- Manufacturing costs expected less than honey-comb
- large misalignment capability

Disadvantages:

- Greater contribution to impedance
- Transition to oval cross-section

Conclusion

The CERN vacuum group has undertaken a series of developments in UHV technologies:

- SMA connectors is a mature technology for UHV applications. Implementation study to FCC-ee has been initiated as well as the verification of its suitability to respond to the FCC-ee particularities.
- Radiation hard permanent bake out system is under development. Good progress has been done so far: proof of concept test has been successfully carried out. Further development is required.
- Additive manufacturing of copper by cold spray is in a first exploratory phase. First results are very promising. Further development is required to assess strength, bounding strength, the effect of local heat treatment, bakeout, etc for its validation.

Development will be pursued with sample and prototype manufacturing and testing.

These technologies are expected to be favourably applied to the FCC-ee vacuum system, in particular for the quad vacuum chambers and BPM button integration, the later requiring a close collaboration between VSC and BI teams.

Thanks for your attention.

Thanks to the vacuum team, in particular Christian Duclos, Roberto Kersevan, Hendrik Kos, Marco Morrone, Fabrizio Niccoli and last but not least Samuel Rorison.

Concept of SMA connectors for UHV applications

Heating/mounting

Martensite: stable at <u>low</u> temperature and <u>high</u> stress

Austenite: stable at <u>high</u> temperature and <u>low</u> stress

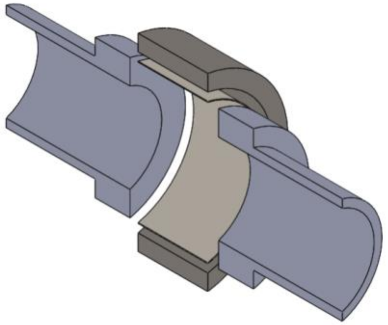

Martensitic enlarged cold-shape

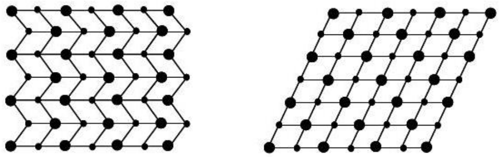

Twinned (low stress) or detwinned (high stress) martensite

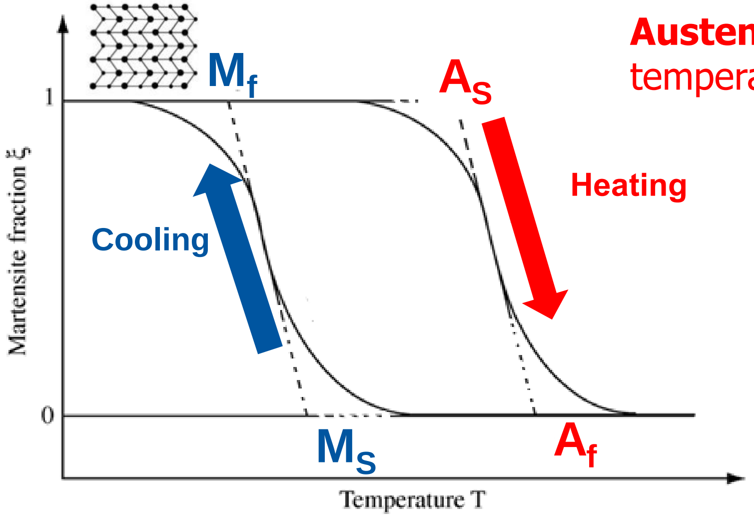

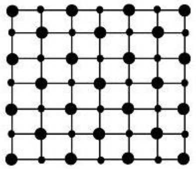

Austenite

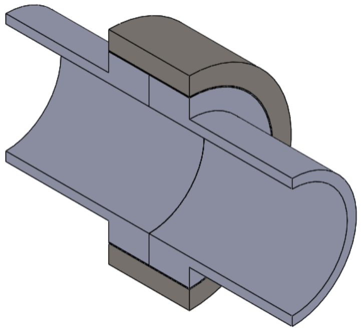

Austenitic contracted hot-shape

Cooling/dismounting

Reversible phase transformation: displacive transformation without diffusion process

- **A_s**: Austenite start temperature
- **A_f**: Austenite finish temperature
- **M_s**: Martensite start temperature
- **M_f**: Martensite finish temperature

Transformation Temperatures (TTs) depend on:

- Chemical composition
- Internal stress/strain field (dislocation arrays/precipitates)
- Thermo-mechanical cycling

Advantages and potential applications

- A compact, leak tight and easily mountable\dismountable connection system, compatible with accelerator environment:
  - Magnetic permeability < 1.002
  - Thermal outgassing < 10^{-13} mbar.l^{-1}.s^{-1}.cm^{-2}
  - Radiation hard (up to 4 MGy at least)
- Possibility of remote controlling\activation
- Possibility to connect dissimilar materials
- Possibility to use in high demanding areas (e.g. collimator areas, machine/detector interface)

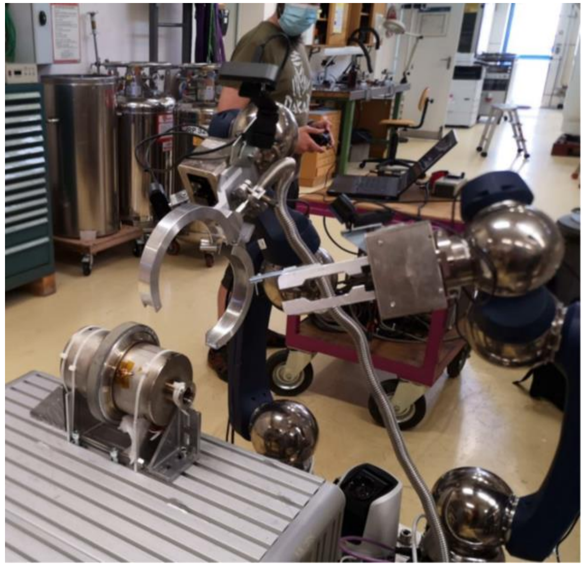

Declamping with a robot

LHC dump windows

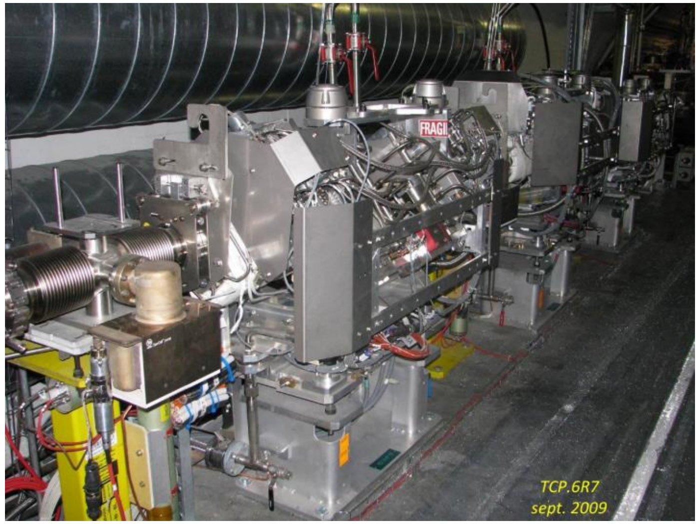

LHC collimators

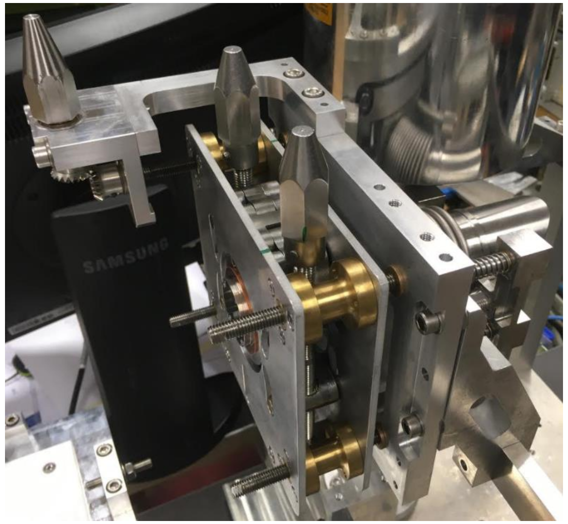

Vacuum module for the MDI area

Principle of Cold Spray

1D isentropic flow equations:

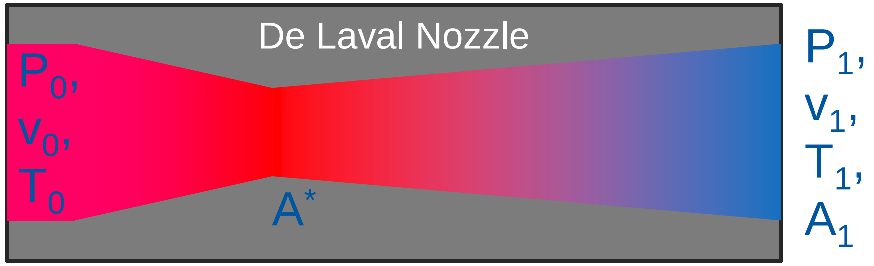

$$\frac{P_0}{P_1} = \left(1 + \frac{\gamma - 1}{2} M_1^2\right)^{\frac{\gamma}{\gamma-1}}$$

$$\frac{T_0}{T_1} = 1 + \frac{\gamma - 1}{2} M_1^2$$

$$M_1 = \frac{v_1}{c_1} = \frac{v_1}{\sqrt{\gamma R_s T_1}}$$

$$\frac{A_1}{A^*} = \frac{1}{M_1}\left[\frac{2}{\gamma + 1}\left(1 + \frac{\gamma - 1}{2} M_1^2\right)\right]^{\frac{\gamma+1}{2(\gamma-1)}}$$

$$\gamma = \frac{c_p}{c_v}$$

γ=5/3 (1.67) for monoatomic perfect gas
γ=7/5 (1.4) for diatomic perfect gas and
γ=1,33 for polyatomic perfect gas

R_s is the specific gas constant given by R/M_{molar}

Nitrogen is commonly used. Helium is used to reach higher velocity.

Bounding mechanism

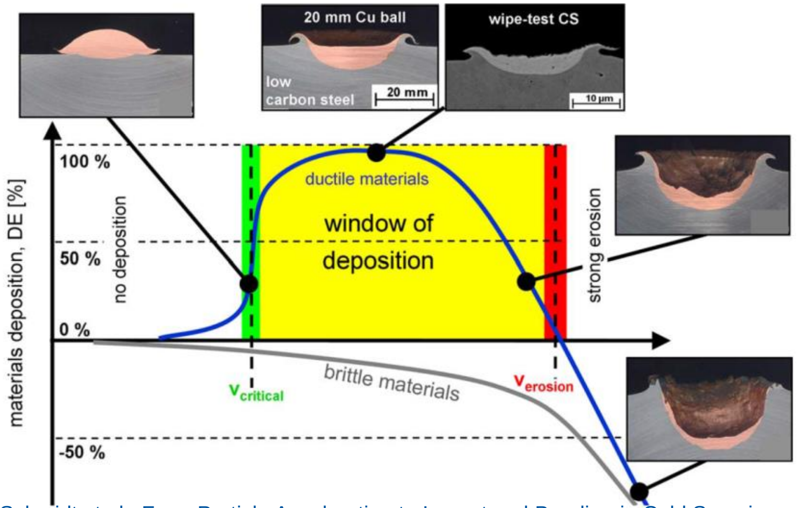

T. Schmidt et al., From Particle Acceleration to Impact and Bonding in Cold Spraying, Journal of Thermal Spray Technology, 18, 5-6, 794-808, 2009

Table 1 Values of critical velocity for bonding assuming a particle size of 20 µm

Material	Melting point, °C	Critical velocity, m/s
Aluminium	660	620-660
Titanium	1670	700-890
Tin	232	160-180
Zinc	420	360-380
Stainless steel (316L)	1400	700-750
Copper	1084	460-500
Nickel	1455	610-680
Tantalum	2996	490-650

Typical surface around the critical velocity

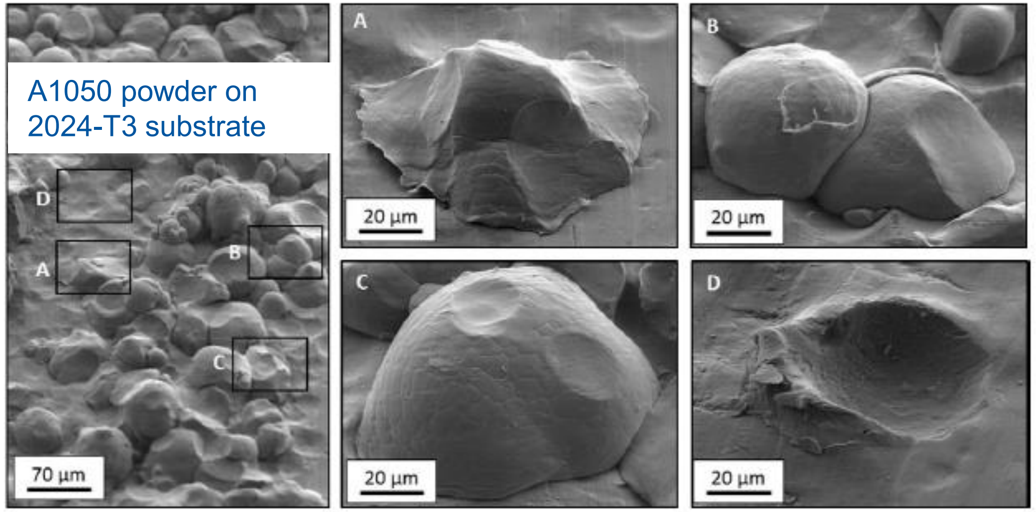

Q. Blochet, Influence of substrate surface roughness on cold-sprayed coating-substrate bond strength in aluminum-based systems, PhD Thesis, Mines ParisTech, 2015

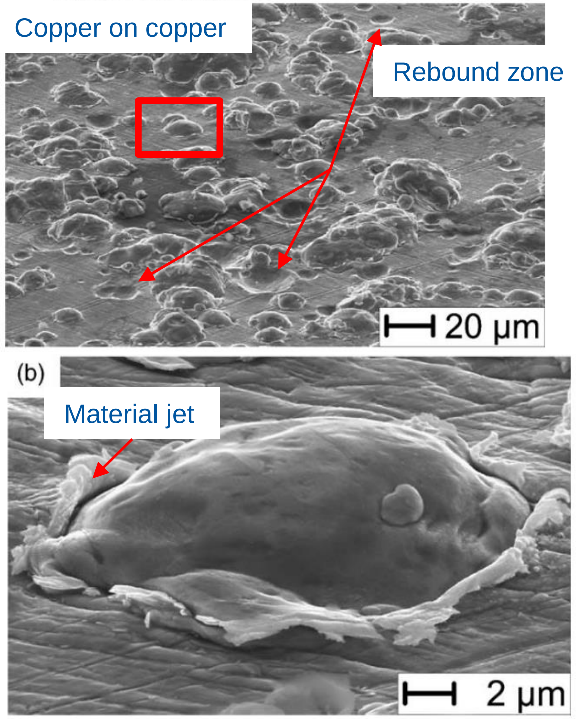

Assadi et al., Bonding mechanism in cold gas spraying, Acta Materialia, 51, 4379-4394, 2003

Some properties: example of copper

Electrical conductivity

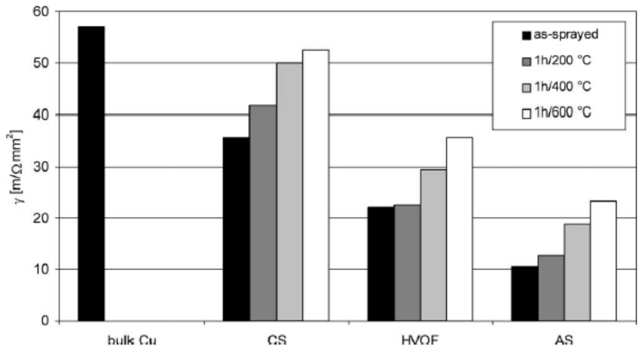

Fig. 9. Conductivity of Cu-coatings processed by cold spraying, HVOF spraying and arc spraying in the as-sprayed state and after different annealing conditions. Annealed bulk Cu serves as reference material.

T. Stoltenhoff et al., Microstructures and key properties of cold-prayed and thermally sprayed copper coatings, Surface & coatings Technology, 200, 2006

Bounding strength

With helium

Coating material	Substrate material	Substrate preparation	Bond strength		Reference
Cu	Aluminum	Grit blasting	30–35	ASTM C-633	Taylor et al. (2006)
Cu	Copper, AA5052, AA6063		> 150	Modified tensile test	Huang and Fukanuma (2012)

With nitrogen

Cu	Copper	Grit blasting	17	JIS H 8664	Fukanuma and Ohno (2004)
Cu	Aluminum	Grit blasting	24	JIS H 8664	Fukanuma and Ohno (2004)
Cu	Aluminum	Grit blasting	> 40	ASTM C-633	Gärtner et al. (2006)
Cu	Steel	Grit blasting	10–20	ASTM C-633	Gärtner et al. (2006)
Cu	Aluminum, Copper	Grit blasting	40	EN 582	Stoltenhoff et al. (2006)
Cu	Steel	Grit blasting	10	EN 582	Stoltenhoff et al. (2006)
Cu	Copper, AA5052, AA6063		> 100	Modified tensile test	Huang and Fukanuma (2012)
$Cu+Al_2O_3$	Copper, steel	Grit blasting	20–23	EN582	Koivuluoto et al. (2008a, b)

After Jeandin et al., Coating properties in Modern cold spray, Ed. J. Villafuerte, Springer, 2015

Coating strength

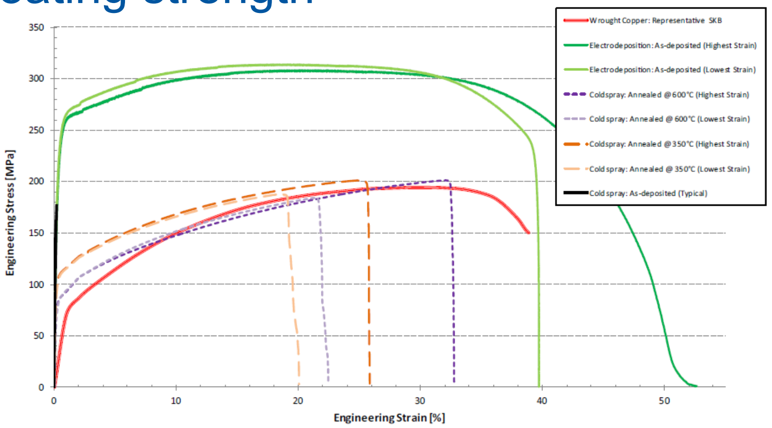

C.H. Boyle, Mechanical performance of integrally bounded copper coatings for the long term disposal of used nuclear fuel, Nuclear Engineering and design, 293, 2015

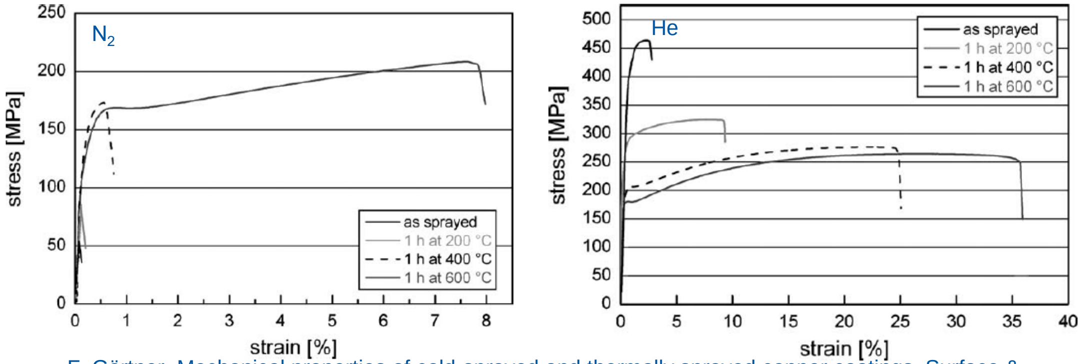

F. Gärtner, Mechanical properties of cold-sprayed and thermally sprayed copper coatings, Surface & Coatings Technology 200, 2006

→ Material properties are affected by the cold spray process but they can significantly be recovered by dedicated post treatment.

Application to FCC

FCC-hh beam screen

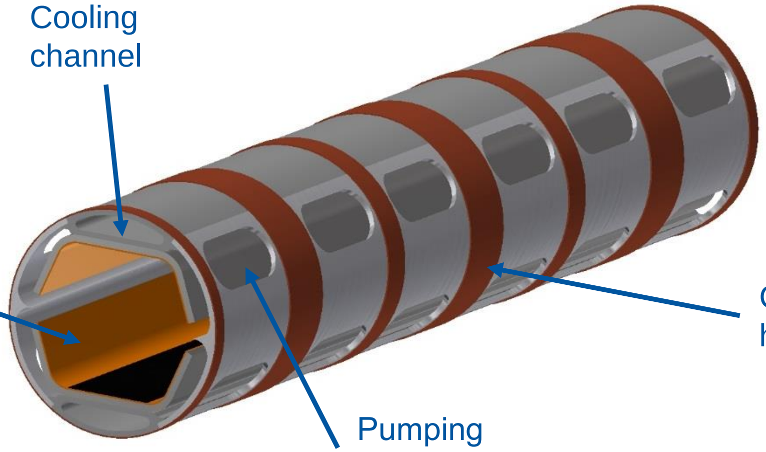

Requirements:

- Copper material (thermal conductivity)
- Stainless steel substrate
- Discountinuous (longitudinally → reduced Lorentz forces during a magnet quench)
- Continuous as close as possible to the cooling channel (better cooling and temperature control)
- Done after beam screen assembly (welds)
- No spray or coating contamination inside the beam screen
- Industrial process

A technology successfully applied in Accelerators

Local coating:

Heat transfer:

Copper trips on FCC-hh beam screen prototype.

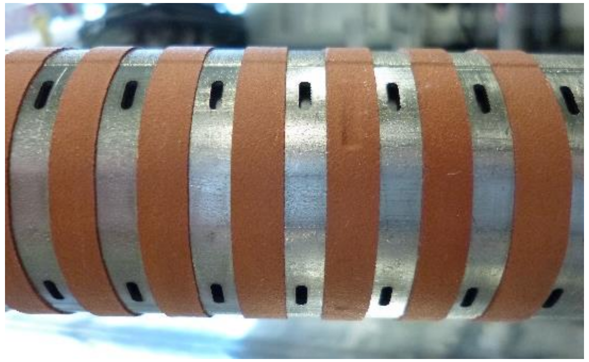

Electrode:

- Measurement of electrons for the FCC-hh beam screen prototype experiment at ANKA.
- Clearing electrode (optimisation of ceramic layer required for non-baked system).

Copper and aluminium cold spray coating on ceramic insulated copper coated stainless steel sheet

Application to FCC beam screen

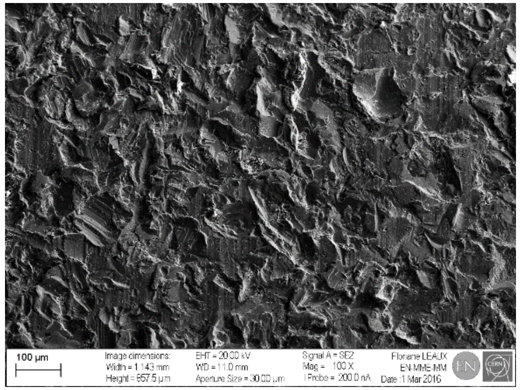

Surface preparation by blasting (Al2O3)

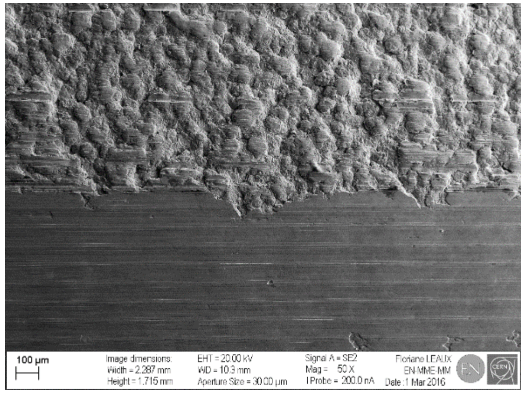

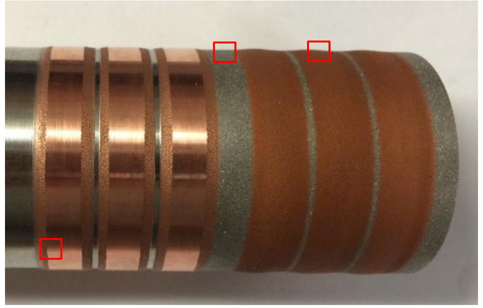

Cold sprayed copper on austenitic stainless steel.

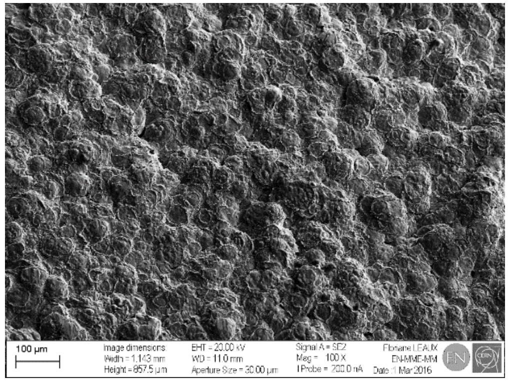

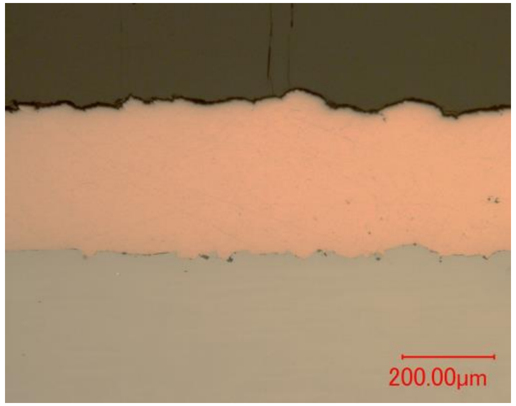

Possible improvements:

- Surface preparation: laser treatment
- Nozzle geometry: correct width
- Process parameters

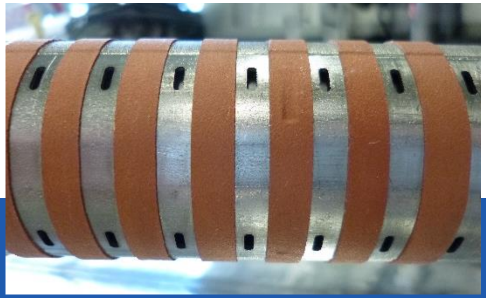

Study of the ceramic layer

Samples with different ceramics, ~ 0.5 mm thick, plasma sprayed on copper plates, have been manufactured:

- Al_2O_3 99%
- Al_2O_3 – 13 TiO_2
- Cr_2O_3 – 4 SiO_2 – 3 TiO_2
- ZrO_2 – 8Y_2O_3

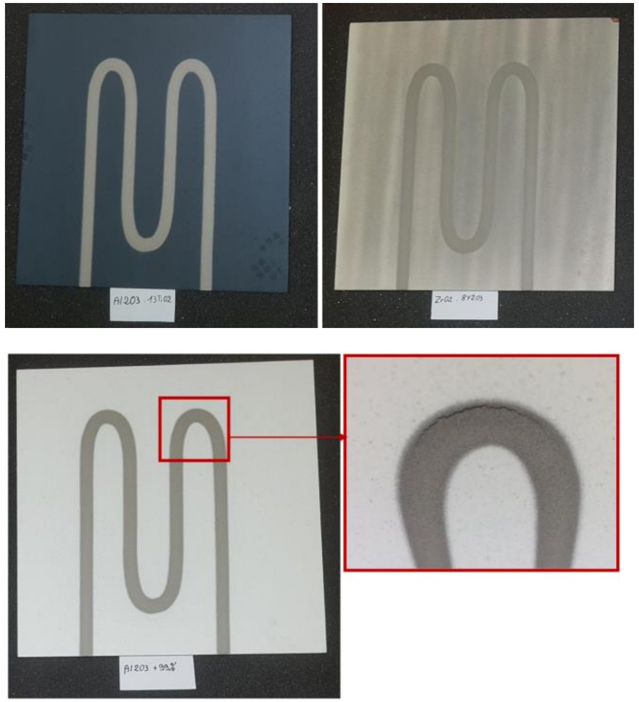

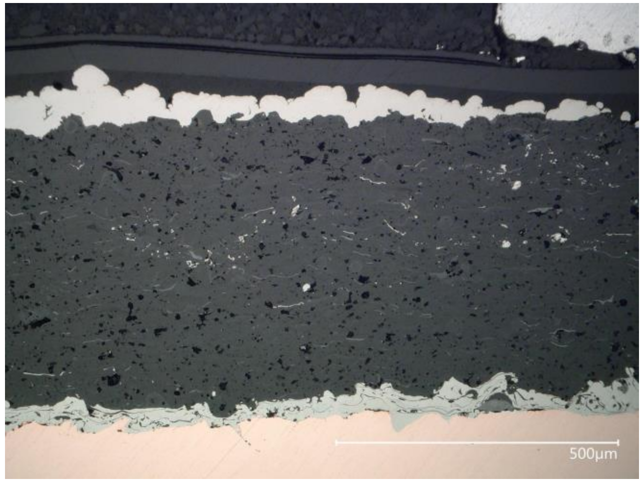

Al2O3+13TiO2

The different ceramic layer revealed different adhesion quality of the Ti track.

Residual stresses

Residual stresses have been assessed by hole drilling method, on the ceramic and on the track.

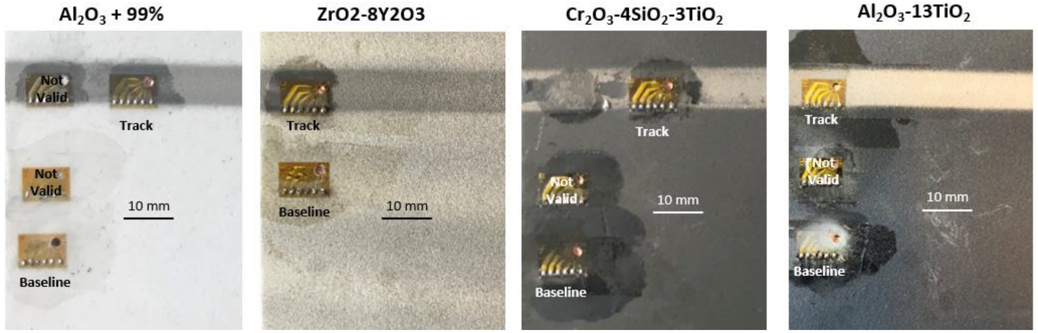

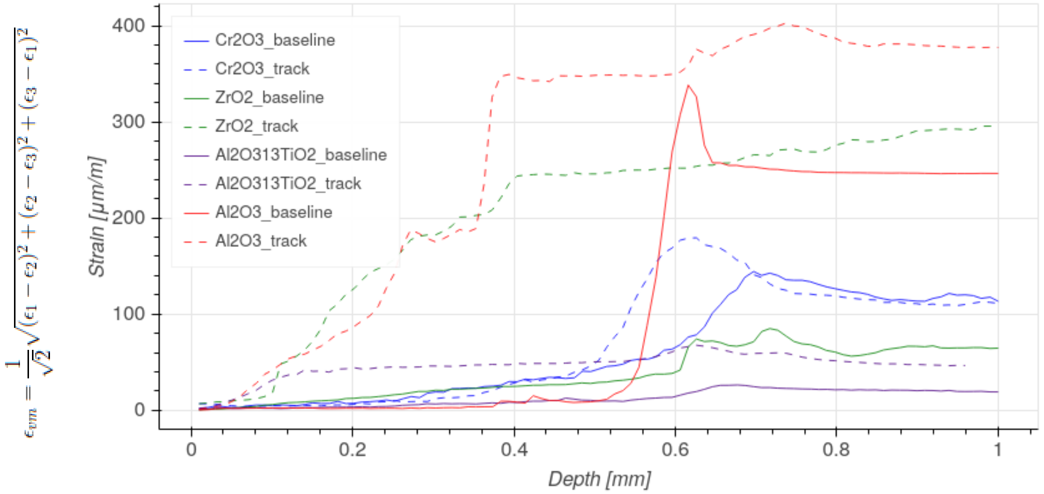

Comparative strain measurements

Significant difference is observed between the different ceramics. Al_2O_3-13TiO_2 exhibits the lowest residual stress, in the 10 MPa range.

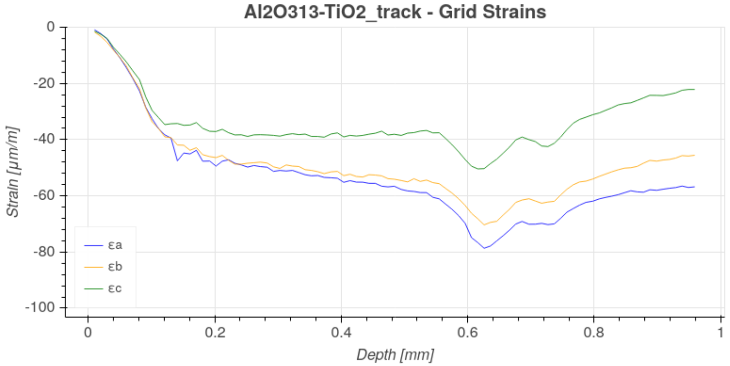

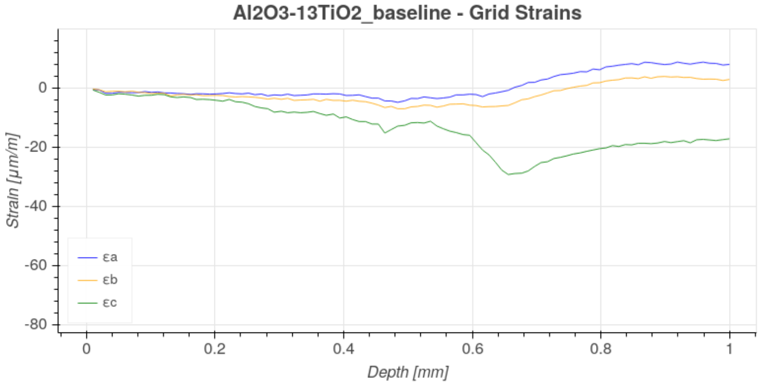

Strain measurements for Al_2O_3-13TiO_2 ceramic layer

Functional tests have been successfully carried out on the Al_2O_3-13TiO_2 plate, including 50 thermal cycles to 250 °C.

Al_2O_3 + 99%

Cr_2O_3-4SiO_2-3TiO_2

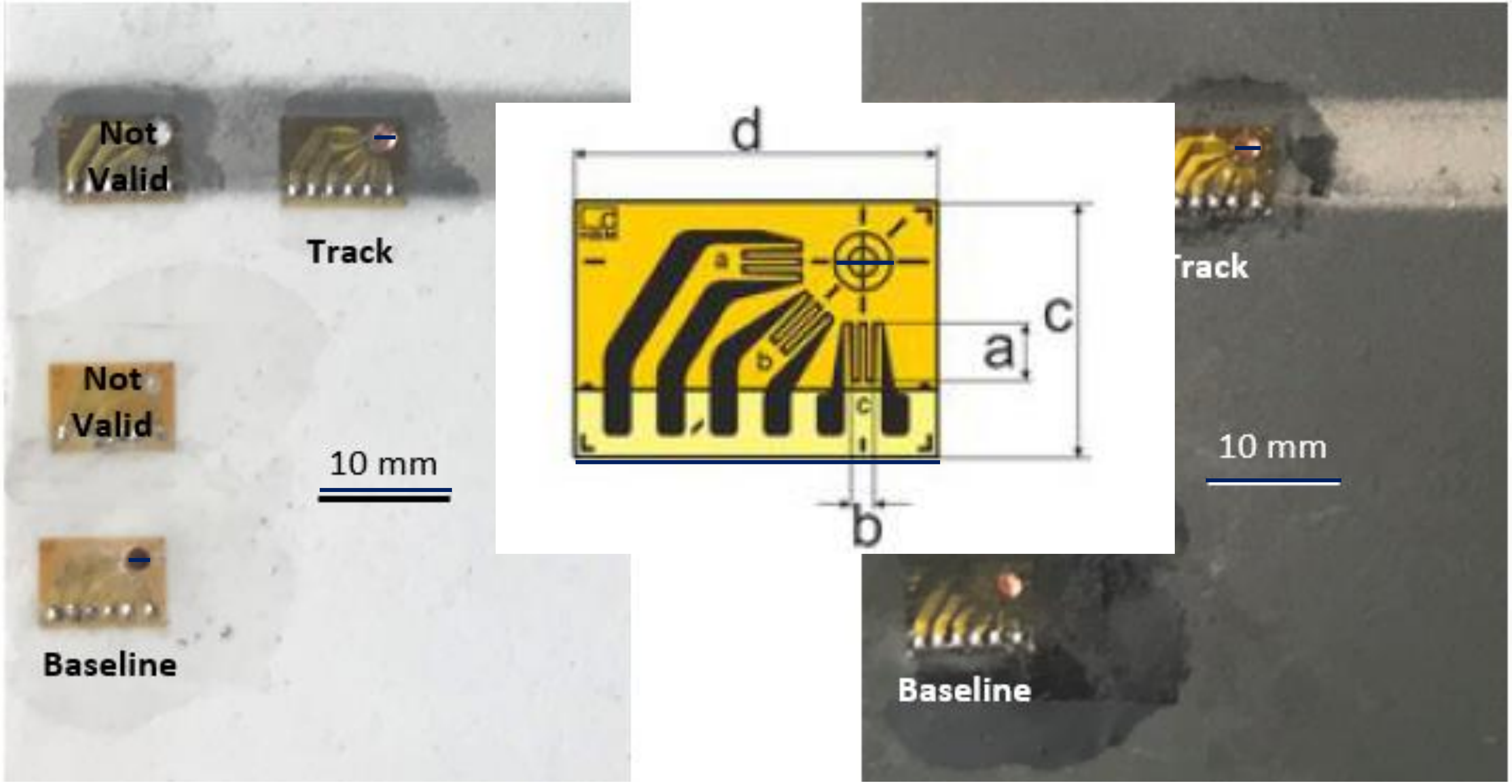

40

Prototype – Proof of concept

Some further developments are required:

1. Thickness irregularities have been observed in the corners of the track (different speed of the gun) → cold spots (thicker) and hot spots (thinner).

→ Better management of the robot displacement required.
→ Tests of different track U turn paths.

Thickness irregularities

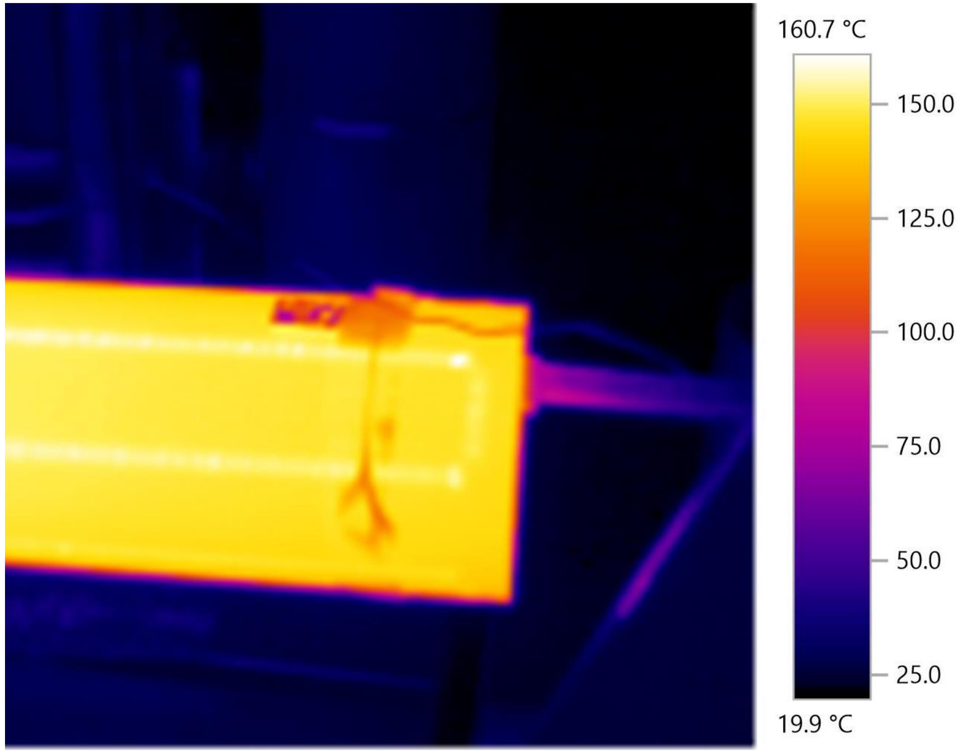

Hot/cold spots induced by thickness irregularities

2. Measurements of the electrical resistance is not in agreement with expected value → measurement of resistivity of cold sprayed material ongoing.
3. Electrical connections to be defined for a safe operation.